

M Z-TH /05-17
hep-ph/0508173
August 2005

Evaluating massive planar two-loop tensor vertex integrals

Stefan Grosse^{1,2} and Markus M. Kerner¹

¹ Institut für Physik der Johannes-Gutenberg-Universität,
Staudinger Weg 7, 55099 Mainz, Germany

² Füüsika-Kemiteaduskond, Tartu Ülikool, Tähe 4, 51010 Tartu, Estonia

Abstract

Using the parallel/orthogonal space method, we calculate the planar two-loop three-point diagram and two rotated reduced planar two-loop three-point diagrams. Together with the crossed topology, these diagrams are the most complicated ones in the two-loop corrections necessary for instance for the decay of the Z^0 boson. All integration steps up to the last two ones are performed analytically and will be implemented under *χloops* as part of the Mainz *χloops*-GNAC project. The last two integrations are done numerically using methods like VEGAS and Divonne. Thresholds originating from Landau singularities are found and discussed in detail. Finally, we calculate the diagrams for different physical processes and for the general mass case and demonstrate the reliability of the results. Our results can easily be generalized to the case of the crossed topology.

1 Introduction

Precision measurements at the LEP collider at CERN and other colliders like e.g. SLAC at SLAC, TEVATRON at Fermilab and HERA at DESY have reached a precision which has exceeded all expectations. This is true especially for electron colliders [1, 2, 3, 4]. In moment the precision of measurements related to the parameters of the standard model of electroweak interactions reaches values up to $O(10^{-4})$ [4]. At future colliders like the LHC or the ILC (including GigaZ), further distinct improvements are expected [3, 5, 6, 7, 8].

Compared to this, theoretical predictions accomplish this precision only in very few cases. To check the validity of the standard model and to be able to draw conclusions about "new physics", progress in theoretical methods and their application is necessary [2, 3]. The complexity of the calculations and the number of the graphs which have to be calculated within perturbation theory grows considerably order by order. At second order only a few observables are calculated [9]. Still there is no method available which allows for the (semi)automatic calculation of arbitrary processes at this order. Much work has been done on NNLO calculations [10, 11, 12, 13, 15, 16, 14, 17, 18, 19, 20]. However, for evaluating two-loop three-point diagrams in the general mass case only the methods proposed in Refs. [21, 22, 23] have been used successfully. With increasing energy as it will be used at the ILC, radiative corrections will become increasingly important. Therefore, there is still need for independent methods to calculate general massive two-loop vertex diagrams.

The planar and rotated reduced planar ladder two-loop three-point diagrams in the general massive case are necessary e.g. for calculations like the NNLO-corrections to the effective weak mixing angle $\sin^2 \theta_e^{\text{lept}}$ [24, 25] and other processes like $Z^0 \rightarrow t\bar{t}$. For our calculations we use the parallel/orthogonal space method [26] which allows to separate effects coming from inner momenta from those of momenta of the outer particles of the process. We present a tensor reduction which reduces the mentioned topologies containing an arbitrary tensor structure to a set of master integrals with strongly restricted numerator structure [27]. Because most of the integration steps can be performed analytically, the Landau singularities of the Feynman diagrams can be related graphically to the integrands in the remaining two-dimensional integration region. Using different algorithms, we demonstrate the numerical stability. For the remaining basic integrals which are not considered, we refer to already established methods [10, 28, 29, 30, 31].

For the planar and rotated reduced planar topologies the algorithm for the numerical

calculation of the last two integrations in the general mass case is developed and its reliability is demonstrated. In addition, further exhaustive numerical tests are done. While for the numerical integration programs like the Monte Carlo integration routine VEGAS [32, 33] and the program Divonne of the library CUBA [34] are used, the implementation of the algorithms for the semi-automatical calculation in *χloops* [35, 36, 37] is part of the work described in this paper. In the *χloops*-GINAC project developed by the members of the THEP working group in Mainz [39], the automatic generation of Feynman diagrams and their calculation with analytical and numerical means is scheduled. For this purpose the language for algebraic calculation GINAC was developed [40]. While most of the basic two-loop integrals not considered in this paper are already implemented in *χloops*, the missing planar topologies will be added in the course of the work introduced here.

The paper is organized as follows. In Sec. 2 we introduce the main tools of the analytical calculation associated with the P/O-method. The tensor reduction procedure is explained in detail in Sec. 3 for the non-reduced planar two-loop three-point diagram, and modifications in case of the rotated reduced planar diagrams are mentioned and explained. The tensor reduction leads to basic integrals which are integrated analytically in Sec. 4 up to the last two integrations. In Sec. 5 we deal with the analysis of Landau singularities and thresholds. Sec. 6 is devoted to the numerical integration. In both sections we present examples to show the reliability of our procedure. In Sec. 7 we give our conclusions.

2 Tools for the calculation

In this section we provide the reader with the tools necessary for the calculation of massive two-loop tensor vertex integrals. Most of the tools were already introduced in the literature [26, 41, 42, 43, 44, 45, 46]. Therefore, we can be brief in presenting these tools.

2.1 The parallel/orthogonal space method

The integrals we have to calculate are determined by the two momenta of the produced particles, p_1 and p_2 . Because the integrals are expressed in terms of covariant quantities, we are free to decompose any loop momentum k into two covariant vectors, $k = k_\parallel + k_\perp$, where k_\parallel has components in the parallel space which is the linear span of the external momenta p_1 , while k_\perp is the orthogonal complement with $k_\perp \cdot p_1 = 0$ with components

in the orthogonal space. For three-point functions we can consider the process in the rest frame of the decaying particle. In this frame the two emerging particles are produced back-to-back, defining the z-axis.¹ In this frame the representation

$$p_1 = (E_1; \mathbf{q}; 0; 0); \quad p_2 = (E_2; -\mathbf{q}; 0; 0); \quad p = p_1 + p_2 = (E; 0; 0; 0) \quad (1)$$

can be used where p is the momentum of the decaying particle with $E = E_1 + E_2$ and $p^2 = E^2$. Accordingly, the loop momenta k and l necessary for the description of the two-loop integral are parametrized by [42]

$$k = (k_0; k_1; \mathbf{K}_\perp); \quad l = (l_0; l_1; \mathbf{L}_\perp); \quad (2)$$

The two-dimensional vectors \mathbf{K}_\perp and \mathbf{L}_\perp are represented in polar coordinates, using the length squared $s = \mathbf{K}_\perp^2 = k_\perp^2$ and $t = \mathbf{L}_\perp^2 = l_\perp^2$ and two angles, the angle θ of \mathbf{K}_\perp with the x-axis and the relative angle ϕ . We can write

$$\mathbf{K}_\perp \cdot \mathbf{L}_\perp = k_\perp l_\perp z = \frac{P}{stz}; \quad z = \cos \phi = \cos(\mathbf{K}_\perp; \mathbf{L}_\perp); \quad (3)$$

The choice of parallel and orthogonal subspaces itself is Lorentz invariant, so that the calculation can still be done in any Lorentz frame. The benefit of the parallel/orthogonal space method (P/O-space method) is that the contributions belonging to the orthogonal space can be integrated out and we are left with the contributions in parallel space only. The integration measure is accordingly written as

$$d^4k \, d^4l = \int_0^z dt ds \int_{-1}^{z+1} dk_0 dl_0 dl_1 dk_1 \int_{-1}^{z+1} \frac{dz}{1-z^2} \quad (4)$$

where the trivial integration over z is already performed.

2.2 The linearization

The denominators of integrals occurring in two-loop calculations contain up to six propagator factors. A typical factor is given by

$$P_1 = (k - p)^2 - m_1^2 + i \quad (5)$$

where $\epsilon > 0$. In P/O-space representation this propagator factor reads

$$P_1 = (k_0 - E_1)^2 - (k_\perp - \mathbf{q})^2 - k_\perp^2 - m_1^2 + i; \quad (6)$$

¹Breaking conventions, the z-component will be written as the second component in the following.

If we replace $k_0 = k_0^0 + k_1$, we obtain

$$P_1 = (k_0^0 + E_1)^2 - 2k_1(k_0^0 + E_1) + k_1^2 - m_1^2 + i \quad (7)$$

where k_1 no longer appears quadratically. This replacement, also known as linearization, is allowed because the integral ranges for k_0 and k_1 are going from -1 to $+1$. However, because of the occurrence of the mixing propagator factor

$$P_3 = (k + l)^2 - m_3^2 + i; \quad (8)$$

the signs for the linearizations in k and l are coupled. In applications of this linearization we use the sign which is most appropriate for our aims. The benefit of the linearization is that the integrals over k_1 and l_1 can then be calculated by using the residue theorem.

2.3 The integration over z

The quantity z occurs only in the just mentioned propagator factor P_3 . After linearization this propagator factor can be written as $P_3 = A + Bz + i$ where

$$A = (k_0^0 + l_0^0)^2 - 2(k_1 + l_1)(k_0^0 + l_0^0) - (s + t) - m_3^2; \quad B = \frac{p - s}{2st} \quad (9)$$

P_3 occurs only once in the denominator (if at all). The resulting integral

$$\int_{-1}^{+1} \frac{dz}{z^2} \frac{1}{A + Bz + i} = \frac{1}{c} \frac{1}{(A + i)^2} - \frac{1}{c} \frac{1}{B^2} = \frac{1}{c} \frac{1}{(A + i)^2} - \frac{1}{4st} \quad (10)$$

can be written in this closed form only if we make a convention different from the usual one. We stipulate that the cut of the square root is found on the positive real axis instead of the negative one. For this reason we added the index "c" which reminds of the different cut. The occurrence of the modified square root has consequences for the integrations to follow because in closing paths for the residue theorem we have to avoid crossing this cut. In order to find conditions for this we split the square root up into a product of two square roots $\sqrt{c} \sqrt{A + B + i}$. If one of the radicands is equal to a positive real number x , we are definitely crossing the cut. Written in terms of k_1 and l_1 , we obtain

$$(k_1 + l_1)^{\text{cut}} = \frac{x - (k_0^0 + l_0^0)^2 + m_3^2 + \left(\frac{p - s}{2}\right)^2 - i}{2(k_0^0 + l_0^0)}; \quad (11)$$

Note that the two undetermined signs are not correlated. While the sign between $\frac{p - s}{2}$ and $\frac{p - t}{2}$ depends on which of the two square roots is taken, the global sign of the right hand side

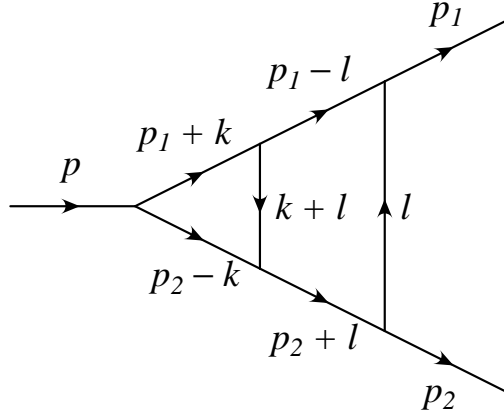


Figure 1: Momentum flow convention for the planar two-loop three-point function

is due to the sign of the linearization. Considering only the linearizations $k_0 = k_0^0 + k_1$, $l_0 = l_0^0 + l_1$, the signs of real and imaginary part of the cut still depend in the sign of $(k_0^0 + l_0^0)$. If $(k_0^0 + l_0^0) > 0$, the cut is located in the lower complex halfplane, the real part starts (for $x = 0$) at some finite value and runs to $+1$, independent of which square root we selected. In order to avoid the cut, we therefore have to close the integration path for k_1 resp. l_1 in the upper complex halfplane while for $(k_0^0 + l_0^0) < 0$ we have to close in the lower halfplane. The situation is the opposite one for the linearization with minus sign.

3 Tensor reduction

After having introduced the main tools for the calculation, we can start with the calculation itself. The starting point is the tensor integral

$$T_{a_0 a_1 a_2 b_0 b_1 b_2 c}^0 = \int \frac{k_0^{a_0} k_1^{a_1} (k_2^2)^{a_2} l_0^{b_0} l_1^{b_1} (l_2^2)^{b_2} (k_2 \cdot l_2)^c}{P_1 P_2 P_3 P_4 P_5 P_6} d^4 k d^4 l \quad (12)$$

where

$$\begin{aligned} P_1 &= (k + p_1)^2 & m_1^2 + i & & P_4 &= (l - p_2)^2 & m_4^2 + i \\ P_2 &= (k - p_2)^2 & m_2^2 + i & & P_5 &= (l + p_1)^2 & m_5^2 + i \\ P_3 &= (k + l)^2 & m_3^2 + i & & P_6 &= l^2 & m_6^2 + i \end{aligned} \quad (13)$$

In Fig. 1 we show the momentum flow for the diagram in order to define the momenta. For

the indices $a_i; b_i; c$ we allow non-negative integer values. In performing the tensor reduction the integrals are simplified to integrals with simpler numerator and/or denominator structure.

For one-loop integrals the numerator can always be removed by reduction procedures [47]. For two-loop integrals this need not be the case. In general there are not enough propagator factors to cancel all components of the numerator that occur. For the genuine planar two-loop three-point function all numerator factors related to the second loop momentum l at least can be cancelled. This is not the case for reduced topologies, and it is not the case for the first loop momentum k . The aim of the tensor reduction in general is to reduce the numerator as far as possible so that the integrations can be performed similar to what is done for a trivial numerator [43]. The reduction procedure will be explained in the following.

3.1 Cancellation of the mixed contribution

The first step in the cancellation procedure consist in cancelling powers of the mixed factor $(k_\mu l_\nu z)$. This factor occurs also in the propagator factor P_3 . We can write

$$2k_\mu l_\nu z = N_3 - P_3 \quad (14)$$

where

$$N_3 = k_0^2 - k_1^2 - k_2^2 + l_0^2 - \frac{z}{4} - \frac{z}{4} + 2k_0 l_0 - 2k_1 l_1 - m_3^2 + i \quad (15)$$

Used iteratively, we obtain

$$(k_\mu l_\nu z)^c = \frac{N_3}{2} - \sum_{i=0}^{c-1} \frac{N_3^i}{2^{i+1}} (k_\mu l_\nu z)^{c-i-1} P_3 \quad (16)$$

This iterative formula is necessary because the propagator factor P_3 occurs only once. As applied to the integral, we obtain

$$\int \frac{(k_\mu l_\nu z)^c d^4 k d^4 l}{P_1 P_2 P_3 P_4 P_5 P_6} = \frac{1}{2^c} \int \frac{N_3^c d^4 k d^4 l}{P_1 P_2 P_3 P_4 P_5 P_6} - \sum_{i=0}^{c-1} \frac{1}{2^{i+1}} \int \frac{N_3^i (k_\mu l_\nu z)^{c-i-1}}{P_1 P_2 P_4 P_5 P_6} d^4 k d^4 l \quad (17)$$

where we skipped all the other occurring numerator factors for convenience. The first part is the same planar integral with a different numerator structure. However, the second part no longer contains the mixing propagator factor P_3 . Instead, the diagram factorizes. In

addition, we can conclude that this part vanishes if $c - i - 1$ is odd. The reason is that the integration over z is given by

$$\int_{-1}^1 \frac{z^{c-i-1} dz}{1-z^2} \quad (18)$$

which vanishes if the integrand is odd. In terms of a scheme we can write

$$\text{Diagram 1} \quad (k_0 \cdot z)^c \quad = \quad \text{Diagram 2} \quad + \quad \text{Diagram 3} \quad (19)$$

After having cancelled the mixing part it is irrelevant with which loop momentum we continue. However, we always start with the orthogonal space components.

3.2 Cancellation of k_2^2

The factor $k_2^2 = s$ occurs in the denominator factor P_1 . We can write

$$k_2^2 = N_1 P_1; \quad N_1 = k_0^2 k_1^2 + 2k_0 E_1 - 2k_1 q_2 + E_1^2 - q_2^2 - m_1^2: \quad (20)$$

The iterative formula

$$(k_2^2)^{a_2} = N_1^{a_2} \sum_{i=0}^{a_2-1} N_1^i (k_2^2)^{a_2-i-1} P_1 \quad (21)$$

can be used for the integral to obtain

$$\int^Z \frac{(k_2^2)^{a_2} d^4 k d^4 l}{P_1 P_2 P_3 P_4 P_5 P_6} = \int^Z \frac{N_1^{a_2} d^4 k d^4 l}{P_1 P_2 P_3 P_4 P_5 P_6} \sum_{i=1}^{a_2-1} \frac{N_1^i (k_2^2)^{a_2-i-1}}{P_2 P_3 P_4 P_5 P_6} d^4 k d^4 l: \quad (22)$$

Schematically this reduction reads

$$\text{Diagram 1} \quad (k_2^2)^{a_2} \quad = \quad \text{Diagram 2} \quad + \quad \text{Diagram 3} \quad (23)$$

In the following only the scheme will be shown.

3.3 Replacement of k_1

In anticipation of the linearization we replace the numerator factors k_1 by $(k_0 \cdot k_1 \cdot k_0)$, using

$$k_1^{a_1} = (-1)^{a_1} \sum_{i=0}^{a_1-1} (k_0)^{a_1-i-1} i^{a_1} (k_0 \cdot k_1)^i: \quad (24)$$

While the additional factors $k_0^{a_1-i}$ will be cancelled together with $k_0^{a_0}$ in the next step, the subsequent linearization will replace $(k_0 \cdot k_1)$ by k_0^0 .

3.4 Cancellation of k_0

P_1 and P_2 are the only propagator factors that contain only k and not l . We can combine these both to obtain

$$2E k_0 = N_2 + P_1 P_2; \quad N_2 = p_2^2 \frac{2}{l_1} m_2^2 + m_1^2; \quad (25)$$

An iterative formula can be constructed as before, the reduction reads

$$l_0^2 \quad ! \quad \text{triangle} + \text{triangle with bubble} + \text{triangle with bubble} \quad (26)$$

3.5 Cancellation of l_7^2

In using

$$l_7^2 = N_6 P_6; \quad N_6 = l_0^2 \frac{2}{l_1} m_6^2 + i \quad (27)$$

we can cancel the factors l_7^2 , ending up with the reduction scheme

$$\text{triangle} \quad \left(\frac{2}{l_1}\right)^{b_2} \quad ! \quad \text{triangle} + \text{triangle in circle} \quad (28)$$

3.6 Cancellation of l_1

Because we have three propagator factors which do not contain k , factors l_1 can be cancelled in this case as well, different from the situation for k_1 , without any consequences for the power of l_0 . We use

$$2q_2 l_1 = N_4 + P_4 P_6; \quad N_4 = 2l_0 E_1 \frac{2}{l_1} + m_4^2 m_6^2 \quad (29)$$

to reduce according to the scheme

$$\text{triangle} \quad \frac{2}{l_1} \quad ! \quad \text{triangle} + \text{triangle with bubble} + \text{triangle with bubble} \quad (30)$$

3.7 Cancellation of l_0

Finally, we can cancel the factors l_0 as well, using

$$2E l_0 = N_5 + P_4; \quad N_5 = p_1^2 - p_2^2 - m_4^2 + m_5^2; \quad (31)$$

The reduction scheme reads

$$l_0 \triangle_{123}^{456} = \triangle_{123}^{456} + \text{bubble}_{3} + \text{bubble}_{5} \quad (32)$$

3.8 Summary of the reduction procedure

After performing the reduction procedure, we can collect all the steps into a single one. All diagrams which after reduction procedure are still of the (original) planar topology have a numerator factors $(k_0 \dots k_4)$ in different powers where the maximal power, i.e. the maximal value for k_i , is given by $a_1 + 2a_2 + 2c$. The numerator factors of the diagrams with reduced topology are changed but by no means easier. Nevertheless, because of the different topology, reduction procedures which are known in the literature or which will be explained in the following can be applied. Schematically we write

$$l_0^{a_0} k_1^{a_1} (k_2^2)^{a_2} l_0^{b_0} l_1^{b_1} (l_2^2)^{b_2} (k_3 \cdot l_2 \cdot z)^c \triangle_{123}^{456} = \triangle_{123}^{456} + \text{bubble}_{3} + \text{bubble}_{5} + \text{circle}_{2}^{(1)} + \text{circle}_{2}^{(2)} + \text{circle}_{2}^{(3)} \quad (33)$$

Denoting the topologies by $T^0; T^1; \dots; T^6$ according to the cancelled propagator factor, we can give the following references:

Two-loop three-point functions with two-point subloop, as they are given in our case by the topologies T^1 and T^2 , can be calculated by using dispersion relations [48, 49, 50].

Factorizing topologies like T^3 and T^6 are calculated as a product of the topologies.

What is left are the rotated reduced planar topologies T^4 and T^5 . They can be reduced in a similar manner as the original planar topologies. In the following section we will deal with these topologies and the necessary modifications of the reduction procedure. They are called rotated because in the original reduced planar topology the line crossing the triangle is going horizontally from left to right, connecting the left vertex with the middle of the vertical line on the right.

3.9 Modifications for the rotated reduced planar topologies

For the rotated reduced planar topologies we assume the same numerator factor as for the non-reduced one, $k_0^{a_0} k_1^{a_1} (k_2^2)^{a_2} l_0^{b_0} l_1^{b_1} (l_2^2)^{b_2} (k_2 \cdot l_2 \cdot z)^c$. The procedure is quite the same as in the case discussed before. But because one of the denominator factors P_4 and P_5 is absent, it is not possible to cancel the factors of l_1 as in the previous case. Instead, we anticipate the linearization as in the case of k_1 (and with the same sign) in writing

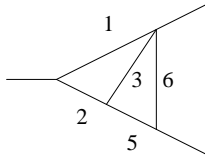
$$l_1 = ((l_0 \cdot l_1) \cdot l_1) \quad l_1^{b_1} = (1)^{b_1} \sum_{j=0}^{b_1} (l_0)^{b_1-j} l_1^j (l_0 \cdot l_1)^j \quad (34)$$

Again, while the additional factors $l_1^{b_1-j}$ will be cancelled together with $l_0^{b_0}$ in the last step, the subsequent linearization will replace $(l_0 \cdot l_1)$ by l_0^0 . However, this last step makes the difference between the two topologies.

For the topology T^4 the denominator factor P_4 is absent. However, we can obtain

$$2(E_2 \cdot q) l_0 = N_5^0 \cdot P_6 + P_5; \quad N_5^0 = 2(l_0 \cdot l_1) q_2 \cdot p_2^2 \cdot m_6^2 + m_5^2 \quad (35)$$

At this point the different signs for the linearization enter the game. While we have designed the term $(l_0 \cdot l_1)$ in the way that it can be combined with the factors from the cancellation of l_1 , in order to obtain l_0 we have to divide by $(E_2 \cdot q)$. However, if the second produced particle is massless, $p_2^2 = 0$, this factor will become zero. In order to include also the massless case, we will prefer the linearization $l_1 = l_1^0 + l_0$ for this topology, i.e. the upper sign. The whole reduction procedure for the case of the topology T^4 reads



$$k_0^{a_0} k_1^{a_1} (k_2^2)^{a_2} l_0^{b_0} l_1^{b_1} (l_2^2)^{b_2} (k_2 \cdot l_2 \cdot z)^c \quad !$$

$$(k_0 + k_1)(l_0 + l_1)$$

$$(36)$$

All the diagrams on the right hand side except for the first one with maximal powers $a_1 + 2a_2 + 2c$ for k and $b_0 + b_1 + 2b_2 + 2c$ for l are again members of the different simpler topology classes which we mentioned in the previous paragraph.

Looking at the topology T^5 , the propagator factor P_5 is absent. In this case we can obtain a reduction formula from combining P_4 and P_6 to obtain

$$2(E_1 - q)l_0 = N_4^0 P_4 + P_6; \quad N_4^0 = 2(l_0 + l_1)q_2 + p_2^2 m_4^2 + m_6^2; \quad (37)$$

In this case the linearization $l_1 = l_1^0 - l_1$ (lower sign) is more appropriate. The result of the reduction reads

$$k_0^{a_0} k_1^{a_1} (k_2^2)^{a_2} l_0^{b_0} l_1^{b_1} (l_2^2)^{b_2} (k_2 \cdot l_2 z)^c \quad !$$

$$(k_0 + k_1)(l_0 + l_1)$$

$$(38)$$

4 Integration of the master integrals

After having reduced the numerator of the integrand to factors $(k_0 - k_1)$ in case of the planar two-loop topology and $(k_0 - k_1)(l_0 - l_1)$ in case of the rotated reduced planar two-loop topologies, we can start to integrate this set of master integrals $T^0; T^x$. Before we do so, we have to consider the occurrence of ultraviolet (UV) divergences and their treatment in terms of appropriate subtractions. As for the treatment of infrared (IR) divergences we refer to Ref. [51] for the scalar case. In the more general case, methods taken from Ref. [52] can be applied. However, in this paper we consider only IR-finite examples.

4.1 Divergences and subtraction procedure

The divergences can be subdivided into three classes: divergences with respect to the two loop momenta and global divergences. It is quite obvious that if we have d_k propagator factors containing only k , d_l propagator factors containing only l , $d_{k,l}$ propagator factors containing both k , l , and a power $k^{n_k} l^{n_l}$ in the numerator, the corresponding degrees of divergence in D space-time dimensions are given by

$$\begin{aligned} \delta_k &= 2(d_k + d_{k,l}) - n_k - D; \\ \delta_l &= 2(d_l + d_{k,l}) - n_l - D; \\ \delta &= 2(d_k + d_l + d_{k,l}) - (n_k + n_l) - 2D; \end{aligned} \tag{39}$$

The two-loop integral is divergent in D dimensions, if at least one of the degrees δ_k , δ_l , or δ is zero or negative. In case of being zero, this divergence is called logarithmic divergence.

In order to calculate the integral, we first have to regularize it. We use dimensional regularization in writing $D = 4 - 2\epsilon$. After that, integrals can be split into a divergent and a convergent part. While the convergent part can be calculated for $\epsilon = 0$, i.e. for $D = 4$ space-time dimensions, the integrand of the divergent part is that simple that it can be integrated analytically.² In an appropriate subtraction procedure, therefore, we subtract and add an integrand which is simple enough to be integrated analytically (at least the singular part) but has the same singularities as the integrand itself in order to cancel the singularities. This subtraction procedure is found and will be formulated

²In the subtraction used here, the divergent part again have to be split into a singular and a non-singular one. The singular part can be calculated analytically, for the non-singular one can again use $\epsilon = 0$.

multiplicatively [27, 46]. For an integrand containing the subtraction factors

$$K^{(j_k)} = \prod_{r=1}^{j_k} \frac{D_k}{D_{k;r}} ; \quad L^{(j_l)} = \prod_{r=1}^{j_l} \frac{D_l}{D_{l;r}} \quad (40)$$

with

$$\begin{aligned} D_k &= \prod_{i=1}^{j_k} (k + p_{k;i})^2 - m_{k;i}^2 + i ; & D_{k;r} &= \prod_{i=1}^{j_k} (k + p_{k;i})^2 - m_{k;i;r}^2 + i \\ D_l &= \prod_{i=1}^{j_l} (l + p_{l;i})^2 - m_{l;i}^2 + i ; & D_{l;r} &= \prod_{i=1}^{j_l} (l + p_{l;i})^2 - m_{l;i;r}^2 + i \end{aligned} \quad (41)$$

where $p_{k;i}; p_{l;i} \in \mathbb{R}; \mathbb{R}^g$, $m_{k;i} \in \mathbb{R}; \mathbb{R}^g$ and $m_{l;i} \in \mathbb{R}; \mathbb{R}^g$, but the subtraction masses $m_{k;i;r}; m_{l;i;r}$ differ from the physical ones and from each other [46],³ the degrees of divergence increase by j_k and j_l , resp. and thus may lead to integrals without singularities for arbitrary values for $r, r, m_{k;i;r}$, and $m_{l;i;r}$. Finally, the limit $r; r \rightarrow 0$ can be performed, leaving the subtracted integral convergent and enabling the semi-analytical calculation. In the end the sum of convergent and divergent integrals have to be independent of the subtraction masses. In the following we will deal with the convergent integral only.

4.2 Subtraction for the planar topology

The result of the reduction procedure explained in the previous section were integrals

$$T^0 = \int \frac{(k_0 - k_1)}{P_1 P_2 P_3 P_4 P_5 P_6} d^4 k d^4 l \quad (42)$$

The degrees of divergence can be calculated in four space-time dimensions,

$$!_k = 2 ; \quad !_l = 4 ; \quad ! = 4 : \quad (43)$$

There are no subdivergences in l . However, for $! = 2$ we have to subtract subdivergences in k . We choose $j_k = 1$ and multiply the integrand in Eq. (42) by

$$K^{(j_k)} = \prod_{i=1}^{j_k} \frac{P_1 P_2}{P_{1;i} P_{2;i}} \quad (44)$$

where $P_1 = (k + p_1)^2 - m_1^2 + i$ and $P_2 = (k - p_2)^2 - m_2^2 + i$ are given in Eq. (13),

$$P_{1;i} = (k + p_1)^2 - m_{1;i}^2 + i ; \quad P_{2;i} = (k - p_2)^2 - m_{2;i}^2 + i : \quad (45)$$

³In the following we will simplify the indices according to the special cases.

Note that each of the subtraction factors in Eq. (44) improves the degree of divergence at least by 1 because by power counting the denominator is given by k^4 and terms of lower order in k while the numerator starts with k^3 . The masses $m_{1,i}; m_{2,i}$ of the subtraction can be chosen arbitrarily. The final result have to be independent of these artificial masses. However, because of technical reasons they are usually chosen to be non-zero and pairwise disjoint [46]. Furthermore, in order not to introduce new thresholds they should be larger than the masses of the decaying particles. On the other hand, they should not be too large because otherwise numerical instabilities could occur.

4.3 Integration for the planar topology

After linearization $k_0 = k_0^0 + k_1$ the propagator factors are given in P/O-representation by

$$\begin{aligned}
P_1 &= 2(k_0^0 + E_1 - \mathbf{q})k_1 + (k_0^0 + E_1)^2 - \mathbf{q}^2 - s - m_1^2 + i \\
P_2 &= 2(k_0^0 - E_2 - \mathbf{q})k_1 + (k_0^0 - E_2)^2 - \mathbf{q}^2 - s - m_2^2 + i \\
P_{1,i} &= 2(k_0^0 - i(E_1 - \mathbf{q}))k_1 + (k_0^0 + iE_1)^2 - i\mathbf{q}^2 - s - m_{1,i}^2 + i \\
P_{2,i} &= 2(k_0^0 - i(E_2 + \mathbf{q}))k_1 + (k_0^0 - iE_2)^2 - i\mathbf{q}^2 - s - m_{2,i}^2 + i : \quad (46)
\end{aligned}$$

In case of the (non-reduced) planar diagram where both linearizations are possible, we select this linearization and $l_0 = l_0^0 + l_1$ for convenience. The propagator factors which are linear expressions in k_1 can be written in compact form,

$$\begin{aligned}
P_1 &= a_1 k_1 + b_1 - s + i ; & P_{1,i} &= a_{1,i} k_1 + b_{1,i} - s + i \\
P_2 &= a_2 k_1 + b_2 - s + i ; & P_{2,i} &= a_{2,i} k_1 + b_{2,i} - s + i : \quad (47)
\end{aligned}$$

Because the parameters a_i can take arbitrary values, the denominator of $K^{(j_k)}$ in Eq. (40) together with the factors P_1 and P_2 from the integrand consists of disjoint linear factors.

Integrating over k_1 , the integration path $[-1; +1]$ can be closed in the upper or lower complex half plane, depending on the sign of the linearization and $(k_0^0 + l_0^0)$ (cf. Eq. (11) and its discussion), and Cauchy's theorem can be applied. The poles are given by the (disjoint) zeros of the propagator factors involved in the calculation. It is easy to see that

$$\begin{aligned}
\text{Res}_{P_1=0}^4 \frac{1}{P_1 P_2} \dot{Y}^k &= \frac{1}{P_{1,i} P_{2,i}} \frac{P_1 P_2}{P_1 P_2} ; P_1 = 0 \Rightarrow \frac{1}{P_2} ; \\
\text{Res}_{P_2=0}^4 \frac{1}{P_1 P_2} \dot{Y}^k &= \frac{1}{P_{1,i} P_{2,i}} \frac{P_1 P_2}{P_1 P_2} ; P_2 = 0 \Rightarrow \frac{1}{P_1} ;
\end{aligned}$$

$$\begin{aligned}
\text{Res}_{P_{1,j}=0}^4 \frac{1}{P_1 P_2} \prod_{i=1}^2 \dot{Y}^k &= \frac{P_1 P_2}{P_{1,i} P_{2,i}} \prod_{i \neq j}^2 \dot{Y}^k ; \\
\text{Res}_{P_{2,j}=0}^4 \frac{1}{P_1 P_2} \prod_{i=1}^2 \dot{Y}^k &= \frac{P_1 P_2}{P_{1,i} P_{2,i}} \prod_{i \neq j}^2 \dot{Y}^k ;
\end{aligned} \quad (48)$$

$P_1 = 0$ results in $k_1 = (s_{1,i})_{i=1}^2 = :k_{1(1)}$, we obtain

$$\frac{1}{P_2}_{P_1=0} = \frac{1}{(s_{2,1}) (s_{2,i})_{i=1}^2} = \frac{N_1^k}{s_{2,1} i}; \quad s_{2,1} = \frac{2 \ 1 \ 1 \ 2}{2 \ 1} : \quad (49)$$

In the same way $P_2 = 0$ results in $k_1 = (s_{2,i})_{i=1}^2 = :k_{1(2)}$, we obtain

$$\frac{1}{P_1}_{P_2=0} = \frac{1}{(s_{1,2}) (s_{1,i})_{i=1}^2} = \frac{N_2^k}{s_{1,2} i}; \quad s_{1,2} = \frac{1 \ 2 \ 2 \ 1}{1 \ 2} : \quad (50)$$

Note that $s_{1,2} = s_{2,1}$. For the other two types of residues, however, a simplification appears after inserting the poles. Because of the fact that for the semi-analytical calculation of the convergent part of the integral we use the limit $i! \rightarrow 0$ for all i , we obtain that

$$i! = 2k_0 = : 0 \quad \text{for } i = 1; 2; \dots; j_k : \quad (51)$$

In this limit and on the pole $P_{1,j} = 0$ or $k_1 = (s_{1,j}, i)_{i=1}^2 = :k_{1(1,j)}$ the different propagator factors read

$$\begin{aligned}
P_{1,i}_{P_{1,j}=0} &= s_{1,i} - s_{1,j}; \\
P_{2,i}_{P_{1,j}=0} &= s_{2,i} - s_{1,j}; \\
P_1_{P_{1,j}=0} &= \frac{1}{0} ((s_{1,0}) (s_{1,i}) + (s_{1,0} - s_{1,1,j})); \\
P_2_{P_{1,j}=0} &= \frac{1}{0} ((s_{2,0}) (s_{2,i}) + (s_{2,0} - s_{2,1,j}));
\end{aligned} \quad (52)$$

Obviously, the dependence on s is found only in the numerator. We can write

$$\frac{1}{P_{2,j}} \prod_{i=1}^2 \dot{Y}^k \prod_{i \neq j}^2 \frac{P_1 P_2}{P_{1,i} P_{2,i}} \prod_{i \neq j}^2 \dot{Y}^k = \sum_{a=0}^{2k-2} N_{1,j;a}^k S^a \quad (53)$$

and similarly

$$\frac{1}{P_{1,j}} \prod_{i=1}^2 \dot{Y}^k \prod_{i \neq j}^2 \frac{P_1 P_2}{P_{1,i} P_{2,i}} \prod_{i \neq j}^2 \dot{Y}^k = \sum_{a=0}^{2k-2} N_{2,j;a}^k S^a : \quad (54)$$

The disjoint poles are given by

$$\begin{aligned}
 k_{1(1)} &= \frac{s_1 - i}{1} & k_{1(2)} &= \frac{s_2 - i}{2} \\
 k_{1(1;i)} &= \frac{s_{1;i} - i}{0} & k_{2(2;i)} &= \frac{s_{2;i} - i}{0} \quad \text{for } i=1;2;\dots;j_k:
 \end{aligned} \tag{55}$$

For $s_i < 0$ ($i = 0;1;2$) the corresponding pole can be found in the upper complex half plane. For the linearization $k_0 = k_0^0 + k_1$ and $k_0^0 + l_0^0 > 0$, the path have to be closed in the upper halfplane. In this case we obtain a non-vanishing residue. For $k_0^0 + l_0^0 < 0$, however, the residue occurs only in case of $s_i > 0$ and has the opposite sign. Using

$$B_n^k = 2^{-i} [(k_0^0 + l_0^0) \theta(-s_n) - (k_0^0 + l_0^0) \theta(s_n)]; \quad n = 0;1;2 \tag{56}$$

where $\theta(x)$ is the step function, we can integrate over k_1 to obtain

$$\begin{aligned}
 & \int_{-1}^{+1} \frac{dk_1}{P_1 P_2} e^{i Y^k} \prod_{i=1}^n \frac{P_1 P_2}{P_{1;i} P_{2;i}} A f(k_1; l_1) \\
 &= \int_{-1}^{+1} \frac{X^2}{s_{1;2}} \frac{B_n^k N_n^k}{i} f(k_{1(n)}; l_1) + \int_{-1}^{+1} \frac{X^{2k} 2^{2k} B_0^k N_{n;i;a}^k}{i} S^a f(k_{1(n;i)}; l_1) A
 \end{aligned} \tag{57}$$

where $f(k_1; l_1)$ is given e.g. by the inverse of $\frac{q}{(A(k_1; l_1) + i)^2}$ 4st.

For the integration over l_1 we have to consider the propagator factors P_4, P_5 , and P_6 . Because the degree of divergence $!_1$ is positive, no subtractions are needed. After the linearization $l_0 = l_0^0 + l_1$ we can write

$$\begin{aligned}
 P_4 &= 2(l_0^0 - E_1 + \alpha_E)l_1 + (l_0^0 - E_1)^2 - \frac{q}{4} - t - m_4^2 + i; \\
 P_5 &= 2(l_0^0 + E_2 + \alpha_E)l_1 + (l_0^0 + E_2)^2 - \frac{q}{4} - t - m_5^2 + i; \\
 P_6 &= 2l_0^0 l_1 + l_0^{02} - t - m_6^2 + i
 \end{aligned} \tag{58}$$

which again can be casted in the closed form

$$P_i = l_1 + i - t + i; \quad i = 4;5;6: \tag{59}$$

The procedure which we explained for the integration over k_1 works accordingly. The poles of

$$\frac{1}{P_4 P_5 P_6} = \int_{-1}^{+1} \frac{Y^6}{(l_1 + i - t + i)^3} \tag{60}$$

are found at

$$l_{1(m)} = \frac{t_m i}{m} \quad \text{for } m = 4; 5; 6: \quad (61)$$

From Eq. (11) we read off that the cut is located in the same complex half plane as for k_1 . Therefore, the occurrence and the sign of the residue is determined by

$$B_m^1 = 2 i [(k_0^0 + l_0^0) \binom{1}{m} - (k_0^0 + l_0^0) \binom{1}{m}]; \quad m = 4; 5; 6: \quad (62)$$

Using Cauchy's theorem, we obtain

$$\begin{aligned} & \int_{-1}^{Z+1} \frac{dl_1}{P_4 P_5 P_6} f(k_{1(n)}; l_1) \\ &= \sum_{m=4}^6 \sum_{j \in m} \binom{1}{j} \binom{1}{m-j} t + i \frac{C}{A} B_m^1 f(k_{1(n)}; l_{1(m)}) \\ &= \sum_{m=4}^6 \sum_{j \in m} \binom{1}{j} \binom{1}{m-j} t + i \binom{1}{m} \frac{C}{A} B_m^1 f(k_{1(n)}; l_{1(m)}): \end{aligned} \quad (63)$$

Of course, the same is valid if $k_{1(n)}$ is replaced by $k_{1(n,i)}$. Usually, j and m are disjoint for $j \notin m$. In this case we can write

$$t \binom{1}{j} \binom{1}{m-j} + i \binom{1}{m} = \binom{1}{j} \binom{1}{m-j} (t_{jm} + i) \quad (64)$$

with

$$t_{jm} = \frac{j m}{j m} : \quad (65)$$

We perform a partial fraction decomposition to obtain

$$\int_{-1}^{Z+1} \frac{dl_1}{P_4 P_5 P_6} f(k_{1(n)}; l_1) = \sum_{m=4}^6 \sum_{j=m+1}^6 \frac{B_m^1 N_{m;j}^1}{t_{mj} + i} f(k_{1(n)}; l_{1(m)}) \quad (66)$$

where $N_{m;j}^1$ are the corresponding coefficients including $\frac{2}{m}$. A special situation occurs if the first produced particle is massless, $p_1^2 = 0$. Because of $q_E = E_1$, in this case we have $q_4 = q_6$ and the corresponding denominator factor contributes by $\binom{1}{4} \binom{1}{6} \frac{2}{6}$ only. However, if the second produced particle is massless, no special situation arises.⁴

⁴For the other linearization $l_0 = l_0^0 - l_1$ the situation is the opposite.

The integrations over k_1 and l_1 and the integration over z can be combined in the closed form expression for the convergent part V^0 of the master integral T^0 in case of $i \neq 0$,

$$V^0 = \int_0^Z \frac{(k_0 \quad k_1)}{P_1 P_2 P_3 P_4 P_5 P_6} K^{(j_k)} d^4 k d^4 l = \int_0^Z \frac{X^2 \quad X^5 \quad X^6}{n=1 \quad m=4 \quad j=m+1} \int_0^Z \frac{k_0^0 dk_0^0 dl_0^0}{t \quad t_{m;j} \quad i} \int_0^Z \frac{N_{m;j}^1 dt}{t \quad t_{m;j} \quad i} + \int_0^Z \frac{B_{n;m}^{k1} N_n^k ds}{(s \quad s_{j2} \quad i)^c (A_{n;m} + i)^2} + \int_0^Z \frac{X^k \quad 2X^2}{i=1 \quad a=0} \int_0^Z \frac{B_{0;m}^{k1} N_{n;j;a}^k s^a ds}{(A_{n;j;m} + i)^2} \quad A \quad 4st \quad 4st \quad (67)$$

where

$$B_{n;m}^{k1} = B_n^k B_m^1 = 4^2 [(k_0^0 + l_0^0) (n) (m) + (k_0^0 + l_0^0) (n) (m)] : \quad (68)$$

and $A_{n;m}$; $A_{n;j;m}$ are the coefficients A in Eq. (9) with k_1 replaced by $k_{1(n)}$; $k_{1(n;j)}$ and l_1 replaced by $l_{1(m)}$, i.e. $A_{n;m} = A(k_{1(n)}; l_{1(m)})$ and $A_{n;j;m} = A(k_{1(n;j)}; l_{1(m)})$.

4.4 Subtraction for the rotated reduced planar topologies

For the rotated reduced planar topologies we are left with integrals

$$T^{9-x} = \int_0^Z \frac{(k_0 \quad k_1) (l_0 \quad l_1)}{P_1 P_2 P_3 P_x P_6} \quad (69)$$

where in case of the topology T^4 ($x = 5$) the upper sign is valid. The degrees of divergence can be calculated to be

$$!_k = 2 \quad ; \quad !_l = 2 \quad ; \quad ! = 2 \quad : \quad (70)$$

For $x = 2$ the integration over l becomes divergent and a subtraction has to be performed in addition to the subtraction in k . The subtraction factor is given by

$$L^{(j_l)} = \prod_{j=1}^{j_l} 1 - \frac{P_x}{P_{x;j}} \quad ; \quad x = 4; 5 \quad (71)$$

where in addition to $P_4 = (1 - p_1)^2 - m_4^2 + i$ and $P_5 = (1 + p_2)^2 - m_5^2 + i$ we have

$$P_{4;j} = (1 - j p_1)^2 - m_{4;j}^2 + i \quad ; \quad P_{5;j} = (1 + j p_2)^2 - m_{5;j}^2 + i \quad : \quad (72)$$

The same limitations apply for the artificial masses $m_{4;j}$ and $m_{5;j}$ as they were mentioned before for the masses $m_{1;i}$ and $m_{2;i}$.

4.5 Integration for the rotated reduced planar topologies

The integration over k_1 can be done in the same way as for the original (non-reduced) planar topology. However, special notes concerning the different linearization in case of the topology T^5 are in order here. For the topology T^5 we have $k_0 = 2k_0^0$ and the step function term B_n^k has to be replaced by

$$B_n^k = 2 \cdot i [(k_0^0 + l_0^0) (n) - (k_0^0 + l_0^0) (n)]: \quad (73)$$

For the integration over l_1 we have to take into account the subtraction. After the linearization $l_0 = l_0^0$ the propagator factors are given in P/O-representation by

$$\begin{aligned} P_5 &= 2 (l_0^0 + (E_2 + \alpha_2)) l_1 + (l_0^0 + E_2)^2 - \alpha_2^2 - t - m_5^2 + i \\ P_{5;j} &= 2 (l_0^0 + j(E_2 + \alpha_2)) l_1 + (l_0^0 + jE_2)^2 - j^2 \alpha_2^2 - t - m_5^2 + i \\ P_6 &= 2 l_0^0 l_1 + l_0^0 t - m_6^2 + i \quad \text{for the topology } T_4; \end{aligned} \quad (74)$$

$$\begin{aligned} P_4 &= 2 (k_0^0 + (E_1 + \alpha_1)) l_1 + (k_0^0 + E_1)^2 - \alpha_1^2 - t - m_4^2 + i \\ P_{4;j} &= 2 (k_0^0 + j(E_1 + \alpha_1)) l_1 + (k_0^0 + jE_1)^2 - j^2 \alpha_1^2 - t - m_4^2 + i \\ P_6 &= 2 k_0^0 l_1 + l_0^0 t - m_6^2 + i \quad \text{for the topology } T_5; \end{aligned} \quad (75)$$

These propagator factors can be written as

$$\begin{aligned} P_x &= x l_1 + x t + i; \quad P_{x;j} = x_{j;j} l_1 + x_{j;j} t + i \quad x = 4;5 \\ P_6 &= l_0^0 l_1 + l_0^0 t + i: \end{aligned} \quad (76)$$

In the limit $l_0^0 \rightarrow 0$ which will be considered in the following, we see that

$$x_{j;j} \rightarrow l_0^0 = 2k_0^0: \quad (77)$$

Integrating over l_1 , in case of the linearization $l_0 = l_0^0 + l_1$ the integration path $[-1; +1]$ can be closed to the upper complex halfplane for $(k_0^0 + l_0^0) > 0$ and to the lower complex halfplane for $(k_0^0 + l_0^0) < 0$. For the other linearization $k_0 = k_0^0$ the situation is just the opposite. Because the poles are given by

$$l_{1(x)} = \frac{t - x}{x} - \frac{i}{x}; \quad l_{1(x;j)} = \frac{t - x_{j;j}}{x_{j;j}} - \frac{i}{x_{j;j}}; \quad l_{1(6)} = \frac{t - l_0^0}{l_0^0} - \frac{i}{l_0^0}; \quad (78)$$

the integration ranges in t are constrained by

$$B_m^1 = \begin{cases} 2 \cdot i [(k_0^0 + l_0^0) (m) - (k_0^0 + l_0^0) (m)] & \text{for } x = 4 \text{ (topology } T^5) \\ 2 \cdot i [(k_0^0 + l_0^0) (m) - (k_0^0 + l_0^0) (m)] & \text{for } x = 5 \text{ (topology } T^4). \end{cases} \quad (79)$$

In order to use Cauchy's theorem, we calculate the residues

$$\begin{aligned}
 \text{Res}_{P_x=0} \frac{1}{P_x P_6} \prod_{i=1}^2 \frac{Y^i}{P_{x,i}} &= \frac{1}{P_6} \prod_{i=1}^2 \frac{P_x}{P_{x,i}}; \\
 \text{Res}_{P_{x,j}=0} \frac{1}{P_x P_6} \prod_{i=1}^2 \frac{Y^i}{P_{x,i}} &= \frac{1}{P_6} \prod_{i=1, i \neq j}^2 \frac{Y^i}{P_{x,i}} \prod_{i=1}^2 \frac{P_x}{P_{x,i}}; \\
 \text{Res}_{P_6=0} \frac{1}{P_x P_6} \prod_{i=1}^2 \frac{Y^i}{P_{x,i}} &= \frac{1}{P_x} \prod_{i=1}^2 \frac{Y^i}{P_{x,i}}.
 \end{aligned} \tag{80}$$

For the first residue we obtain

$$\frac{1}{P_x P_x=0} = \frac{x}{(x-6)(t-t_{x,6}-i)} =: \frac{N_x^1}{t-t_{x,6}-i}; \quad t_{x,6} = \frac{6-x}{6-x} \tag{81}$$

For the second one we first calculate

$$\begin{aligned}
 P_{6, P_{x,j}=0} &= 6 - x_{j,j}; \\
 P_{x, P_{x,j}=0} &= \frac{1}{6} ((x-6)(t-i) - (x_{x,j} - 6x)); \\
 P_{x,i, P_{x,j}=0} &= x_{i,i} - x_{j,j}.
 \end{aligned} \tag{82}$$

Therefore, the numerator of this residuum is independent of t while the denominator is a power series up to the power t^{j-1} . We define the coefficients $N_{x,j;a}^1$ by

$$\frac{1}{P_x P_{x,j}=0} \prod_{i=1, i \neq j}^2 \frac{Y^i}{P_{x,i}} =: \sum_{a=0}^{j-1} N_{x,j;a}^1 t^a \tag{83}$$

The last residue seems to be a combination of a pole in t and a power series. But we can separate these two parts by adding and subtracting an appropriate term. This term is given by

$$\frac{1}{P_x P_6=0} = \frac{6}{(x-6)(t-t_{x,6}-i)} =: \frac{N_6^1}{t-t_{x,6}-i}; \quad t_{x,6} = \frac{x-6}{x-6} \tag{84}$$

If we subtract this term from the result for the last residue, we obtain

$$\frac{1}{P_x} \prod_{i=1}^2 \frac{Y^i}{P_{x,i}} - \frac{1}{P_x} = \frac{1}{P_x} \sum_{i=1}^8 \frac{X^i}{P_{x,i}} + O(P_x^2); \quad \frac{1}{P_x} = \sum_{i=1}^9 \frac{X^i}{P_{x,i}} + O(P_x) \tag{85}$$

The difference no longer has a factor P_x in the denominator. Instead, we obtain again a power series up to the power $t^{\tilde{x}-1}$. We define the coefficients $N_{6;j;a}^1$ by

$$\frac{1}{P_x} \prod_{i=1}^{\tilde{x}} \left(1 - \frac{P_x}{P_{x;i}} \right)_{P_6=0} = \sum_{a=0}^{\tilde{x}-1} N_{6;j;a}^1 t^a \quad (86)$$

Having calculated the residues, we can perform the integration over l_1 to obtain

$$\begin{aligned} & \int_0^Z \frac{dl_1}{P_x P_6} \prod_{i=1}^{\tilde{x}} \left(1 - \frac{P_x}{P_{x;i}} \right) f(k_{1(n)}; l_1) \\ &= \frac{B_x^1 N_x^1}{t \sqrt{t_{x;6}}} \int_0^1 f(k_{1(n)}; l_{1(x)}) + \frac{B_6^1 N_6^1}{t \sqrt{t_{x;6}}} \int_0^1 f(k_{1(n)}; l_{1(6)}) \\ & \quad + \sum_{i=1}^{\tilde{x}-1} \sum_{a=0}^{\tilde{x}-1} B_6^1 N_{x;i;a}^1 t^a + B_6^1 N_{6;i;a}^1 t^a \int_0^1 f(k_{1(n)}; l_{1(6;i)}) \\ &= \sum_{m=x;6}^X \int_0^1 \frac{B_m^1 N_m^1}{t \sqrt{t_{x;6}}} \int_0^1 f(k_{1(n)}; l_{1(m)}) + \sum_{i=1}^{\tilde{x}-1} \sum_{a=0}^{\tilde{x}-1} B_6^1 N_{m;i;a}^1 t^a \int_0^1 f(k_{1(n)}; l_{1(m;i)})^A : \quad (87) \end{aligned}$$

The integrations over k_1 and l_1 and the integration over z can be combined in the closed form expression for the convergent part V^{9-x} of the master integral T^{9-x} in case of $i; i! = 0$,

$$\begin{aligned} V^{9-x} &= \int_0^Z \frac{(k_0 \dots k_{\tilde{x}}) (l_0 \dots l_1)}{P_1 P_2 P_3 P_x P_6} K^{(j_k)} K^{(j_l)} d^4 k d^4 l = \int_0^Z \int_0^1 \int_0^1 k_0^0 dk_0^0 l_0^0 dl_0^0 \int_0^1 ds dt \\ & \quad \sum_{n=1}^X \sum_{m=x;6}^X \frac{B_{n,m}^{k1} N_n^k N_m^1}{(s \sqrt{s_{1;2}} - i)(t \sqrt{t_{x;6}} - i)^c (A_{n,m} + i)^2 4st} \\ & \quad + \sum_{i=1}^{\tilde{x}-1} \sum_{a=0}^{\tilde{x}-1} \frac{X^{j_k} \sqrt{t_{x;6}}^{-2} B_{0,m}^{k1} N_{n;i;a}^k S^a N_m^1}{(t \sqrt{t_{x;6}} - i)^c (A_{n,i,m} + i)^2 4st} \\ & \quad + \sum_{j=1}^{\tilde{x}-1} \sum_{b=0}^{\tilde{x}-1} \frac{X^{j_l} \sqrt{t_{x;6}}^{-1} B_{n;6}^{k1} N_n^k N_{j;b}^1 t^b}{(s \sqrt{s_{1;2}} - i)^c (A_{n,m;j} + i)^2 4st} \\ & \quad + \sum_{i=1}^{\tilde{x}-1} \sum_{j=1}^{\tilde{x}-1} \sum_{a=0}^{\tilde{x}-1} \sum_{b=0}^{\tilde{x}-1} \frac{X^{j_k} X^{j_l} \sqrt{t_{x;6}}^{-2} \sqrt{t_{x;6}}^{-1} B_{0;6}^{k1} N_{n;i;a}^k S^a N_{j;b}^1 t^b}{(A_{n,i,m;j} + i)^2 4st} : \quad (88) \end{aligned}$$

For the topology T^4 ($x = 5$), $B_{n,m}^{k1}$ is given by Eq. (68), i.e. it is the same as for the non-reduced planar topology. For the topology T^5 ($x = 4$), however, we obtain

$$B_{n,m}^{k1} = B_n^k B_m^1 = 4^2 [(k_0^0 + l_0^0) \binom{\tilde{x}}{n} \binom{\tilde{x}}{m} + (k_0^0 + l_0^0) \binom{\tilde{x}}{n} \binom{\tilde{x}}{m}] : \quad (89)$$

The coefficients in the square roots read $A_{n,m} = A(k_{1(n)}; l_{1(m)})$, $A_{n,i,m} = A(k_{1(n;i)}; l_{1(m)})$, $A_{n,m;j} = A(k_{1(n)}; l_{1(m;j)})$, and $A_{n,i,m;j} = A(k_{1(n;i)}; l_{1(m;j)})$.

4.6 Integral basis

The integrals over s and t resulting for both the non-reduced and the rotated reduced planar topology are called basis integrals. They are of the types

$$\begin{aligned}
 F(r_s; r_t; r_0; s_0; t_0) &= \int_0^1 \int_0^1 \frac{ds dt}{(s^2 - i)(t^2 - i)^c (r_0 - r_s - \epsilon t)^2 - 4st}; \\
 F^s(r_s; r_t; r_0; t_0) &= \int_0^1 \int_0^1 \frac{s ds dt}{(t^2 - i)^c (r_0 - r_s - \epsilon t)^2 - 4st}; \\
 F^t(r_s; r_t; r_0; s_0) &= \int_0^1 \int_0^1 \frac{t ds dt}{(s^2 - i)^c (r_0 - r_s - \epsilon t)^2 - 4st}; \\
 F^{st}(r_s; r_t; r_0) &= \int_0^1 \int_0^1 \frac{s t ds dt}{(r_0 - r_s - \epsilon t)^2 - 4st} : \quad (90)
 \end{aligned}$$

All these integrals except for the first one are divergent. However, after the subtraction they occur in sums in which the divergences vanish. While the integral $F(r_s; r_t; r_0; s_0; t_0)$ is calculated in Refs. [44, 45, 53], the other integrals are new. The results in terms of the parameters $r_s, r_t, r_0, s_0,$ and t_0 can be found in Appendix A. In this paragraph we are dealing only with the dependence of the parameters $r_s, r_t,$ and r_0 on the poles found in the residue integration. In case of F we obtain

$$\begin{aligned}
 r_0 &= (k_0^0 + l_0^0)^2 - 2 \frac{n+i}{n} + \frac{m+i}{m} (k_0^0 + l_0^0) - m^2 - i =: r_m; \\
 r_s &= 1 - 2 \frac{k_0^0 + l_0^0}{n}; \quad r_t = 1 - 2 \frac{k_0^0 + l_0^0}{m} \quad (91)
 \end{aligned}$$

where the signs correspond to the two linearizations $l_0 = l_0^0 \pm 1$. For F^s we have to replace n by 0 and n by $n+i$. For F^t we have to replace m by 0 and m by $m+i$. For F^{st} , naturally, both replacements have to be performed. Note that up to the choice for the parameters s_0, t_0, r_s and r_t , F^s and F^t are the same integrals.

We have to consider different cases in order to analyze the analytic behaviour of the square root occurring in the integrand. The equation

$$R(s;t) = (r_0 - r_s - \epsilon t)^2 - 4st = 0 \quad (92)$$

parametrizes an ellipse which separates the positive and negative values of the radicand. Outside of the ellipse the radicand is positive, while for points inside the ellipse it takes negative values. The ellipse touches the axes at $s = r_0 = r_s$ and $t = r_0 = r_t$. For $r_0 < 0$,

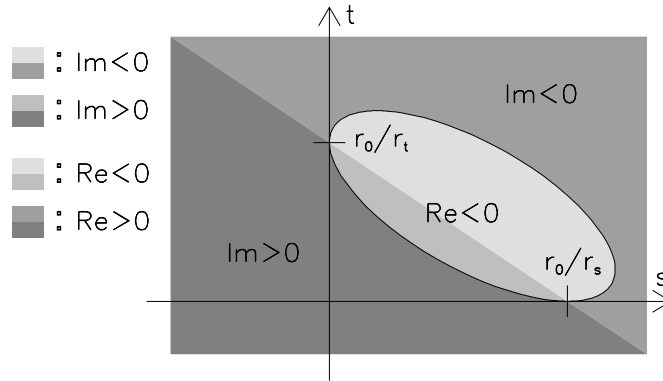


Figure 2: Regions in the $(s;t)$ -plane with different real and imaginary parts for the radicand $R(s;t) = (r_0 - r_s - r_t)^2 - 4st$

therefore, the ellipse is located in the third quadrant. But because the integration is performed in the first quadrant ($s \in [0;1]$, $t \in [0;1]$), the square root will give real values and no imaginary part is produced. For $r_0 > 0$, however, the ellipse moves into the integration region and imaginary parts enter the calculations.

In order to evaluate the square root uniquely, we also consider the imaginary part of the radicand, caused by the term i . It turns out that the sign of the imaginary part is determined by the sign of $r_0 - r_s - r_t$, the zeros of which are given by the straight line connecting the points $s = r_0 = r_s$ and $t = r_0 = r_t$ on the axes where the ellipse touches the axes. Above this line (as seen from the origin for $r_0 > 0$), the imaginary part is negative, below this line it is positive. The situation is shown in Fig. 2.

We distinguish the following cases:

outside the ellipse and below the line ($\text{Re} R(s;t) > 0, \text{Im} R(s;t) > 0$) we have

$$\sqrt[c]{\frac{(r_0 - r_s - r_t)^2 - 4st}{(r_0 - r_s - r_t)^2 - 4st}} = \sqrt[c]{\frac{(r_0 - r_s - r_t)^2 - 4st}{(r_0 - r_s - r_t)^2 - 4st}}$$

outside the ellipse and above the line ($\text{Re} R(s;t) > 0, \text{Im} R(s;t) < 0$) we have

$$\sqrt[c]{\frac{(r_0 - r_s - r_t)^2 - 4st}{(r_0 - r_s - r_t)^2 - 4st}} = \sqrt[c]{\frac{(r_0 - r_s - r_t)^2 - 4st}{(r_0 - r_s - r_t)^2 - 4st}}$$

inside the ellipse ($\text{Re} R(s;t) < 0$) we have

$$\sqrt[c]{\frac{(r_0 - r_s - r_t)^2 - 4st}{(r_0 - r_s - r_t)^2 - 4st}} = i \sqrt[c]{\frac{(r_0 - r_s - r_t)^2 - 4st}{(r_0 - r_s - r_t)^2 - 4st}}$$

The imaginary parts in the rational factors in the numerator, if any, are used to separate real and imaginary part according to the Sokhotsky-Plemely relations

$$\lim_{\epsilon \rightarrow 0^+} \int_a^b \frac{f(x) dx}{x - x_0 - i\epsilon} = P \int_a^b \frac{f(x) dx}{x - x_0} - i \int_a^b \delta(x - x_0) f(x) dx \quad (93)$$

where P indicates the principal value integral.

5 Landau singularities and thresholds

Multiloop integrals with a lot of propagator factors are deeply influenced by their singularity structure. This pole structure can be analyzed by using Feynman parametrization [54, 55]. Starting from

$$F(p_j; m_k) = \int_{\mathbb{R}^L} d^L k_1 \int_{\mathbb{R}^N} \frac{d^N q_n}{A_n} f(p_j; k_1; m_k); \quad A_n = q_n^2 - m_n^2 + i\epsilon \quad (94)$$

with E external momenta p_j , L loop momenta k_l , N internal masses m_n , and q_n a linear combination of p_j and k_l , we can apply the Feynman parametrization

$$\frac{1}{A_1 A_2 \dots A_N} = (N-1)! \int_0^1 \frac{(x_1 + x_2 + \dots + x_N - 1) dx_1 dx_2 \dots dx_N}{(x_1 A_1 + x_2 A_2 + \dots + x_N A_N)^N} \quad (95)$$

By shifting the internal momenta k_l to k_l^0 by finite amounts which are determined by the external momenta, the denominator can be rewritten as

$$D = \int_{\mathbb{R}^N} d^N q_n A_n = K(k_1^0; k_2^0; \dots; k_L^0) \quad (96)$$

where K is independent of internal momenta. It can then be shown that the denominator vanishes, i.e. the integral has so-called Landau singularities, if

$$q_n^2 - m_n^2 = 0 \quad \text{for all } n = 1; \dots; N \quad (\text{first Landau equation}) \quad (97)$$

$$\text{and} \quad \int_{\mathbb{R}^N} d^N q_n = 0 \quad \text{for each loop (second Landau equation):} \quad (98)$$

5.1 Two- and three-particle thresholds

The Landau equations can be used to analyze the given Feynman diagram. For two-point functions, singularities occur if the external momentum crosses thresholds or pseudothresholds. For a sunrise diagram with three different masses, for instance, these thresholds and

pseudothresholds are given by

$$p^2 = (m_1 + m_2 + m_3)^2 \quad (99)$$

where the three-particle threshold is the one for $p^2 = (m_1 + m_2 + m_3)^2$. Only in case of these genuine thresholds the crossing causes the appearance of an imaginary part. According to the Cutkosky rules [56], this imaginary part corresponds to the situation where the particle lines involved are entering the mass shell. In terms of Feynman diagrams, inner lines are broken into outer legs for physical particles. This can be visualized in the Feynman diagram by drawing a cutting line.

In the diagrams we are working with we expect two- and three-particle thresholds. While the two-particle thresholds are related to the values of $s_0 = s_{n,m}$ and $t_0 = t_{n,m}$, all the three-particle thresholds cut the line with mass m_3 and are related to the values of $r_0 = r_{n,m}$,

$$\begin{aligned} s_{1,2} > 0 & , \quad p^2 > (m_1 + m_2)^2; & r_{1,5} > 0 & , \quad p^2 > (m_1 + m_3 + m_5)^2; \\ t_{4,5} > 0 & , \quad p^2 > (m_4 + m_5)^2; & r_{2,4} > 0 & , \quad p^2 > (m_2 + m_3 + m_4)^2; \\ t_{4,6} > 0 & , \quad p^2 > (m_4 + m_6)^2; & r_{1,6} > 0 & , \quad p^2 > (m_1 + m_3 + m_6)^2; \\ t_{5,6} > 0 & , \quad p^2 > (m_5 + m_6)^2; & r_{2,6} > 0 & , \quad p^2 > (m_2 + m_3 + m_6)^2: \end{aligned} \quad (100)$$

5.2 Landau singularities for the scalar topology

As an example we consider the original planar topology in Eq. (42). Because we are only interested in a qualitative analysis, we use the following fictitious values for masses and outgoing momenta not related to any physical process,

$$\begin{aligned} m_1 = 420 \text{ GeV} & \quad m_3 = 100 \text{ GeV} & m_4 = 120 \text{ GeV} & \quad \overline{p_1^2} = 60 \text{ GeV} \\ m_2 = 80 \text{ GeV} & \quad m_5 = 200 \text{ GeV} & m_6 = 300 \text{ GeV} & \quad \overline{p_2^2} = 20 \text{ GeV} : \end{aligned} \quad (101)$$

For the decaying particle, we vary the value of $M = \sqrt{p^2}$ in a range between $M = 100 \text{ GeV}$ and $M = 800 \text{ GeV}$ and plot the real and imaginary part. The result is shown in Fig. 3.

A three-particle threshold is expected for $M = m_2 + m_3 + m_4 = 300 \text{ GeV}$. At this point we see that the imaginary part starts to differ from zero. The two-particle threshold at $M = m_4 + m_5 = 320 \text{ GeV}$ is characterized by a sharp peak in the real part, accompanied by an instant decrease of the imaginary part, leading to a vertical tangent to the curve at this point. For the second two-particle threshold in this energy range at $M = m_1 + m_2 =$

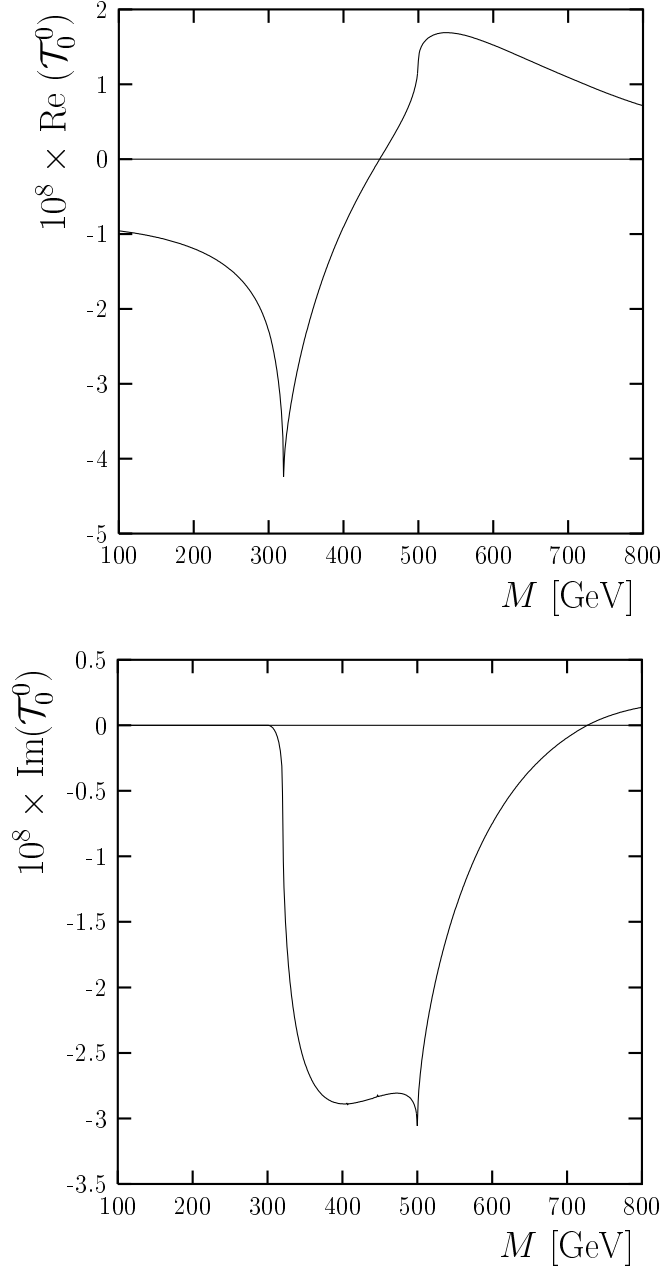


Figure 3: Real part (top) and imaginary part (bottom) for the scalar planar two-loop three-point diagram \mathcal{T}_0^0 of Eq. (42) with decay mass M between 100 GeV and 800 GeV. For the values of masses and momenta we use the standard set given in Eq. (101).

500 GeV, the situation is the opposite. The imaginary part shows a sharp peak while the real part increases with vertical incline.

5.3 The topology of the subtraction terms

If we consider tensor integrals, we have to take subtraction terms into account. As it was shown in the previous section, for the non-reduced planar two-loop three-point master diagram with power $(k_0 - k_1)^2$ we need a single subtraction. Each subtraction replaces the propagator factors by the scaled ones, in our case

$$V_2^0 = \int \frac{(k_0 - k_1)^2 d^4 k d^4 l}{P_1 P_2 P_3 P_4 P_5 P_6} \frac{1}{P_{1;1} P_{2;1}} = \int \frac{(k_0 - k_1)^2 d^4 k d^4 l}{P_1 P_2 P_3 P_4 P_5 P_6} \int \frac{(k_0 - k_1)^2 d^4 k d^4 l}{P_{1;1} P_{2;1} P_3 P_4 P_5 P_6} \quad (102)$$

(for higher subtractions the scaled propagator factors appear in higher powers). If we perform the limit $\epsilon \rightarrow 0$ for $P_{1;1} = (k + p_1)^2 - m_{1;1}^2 - i$ and $P_{2;1} = (k - p_2)^2 - m_{2;1}^2 - i$, the propagator factors lose their dependence on the outer momenta p_i . The momentum scheme given for the original diagram is no longer valid. We first have to perform a partial fraction decomposition for the subtraction term,

$$\int \frac{(k_0 - k_1)^2 d^4 k d^4 l}{P_{1;1} P_{2;1} P_3 P_4 P_5 P_6} = \frac{1}{m_{2;1}^2 - m_{1;1}^2} \int \frac{(k_0 - k_1)^2 d^4 k d^4 l}{P_{1;1} P_3 P_4 P_5 P_6} - \int \frac{(k_0 - k_1)^2 d^4 k d^4 l}{P_{2;1} P_3 P_4 P_5 P_6} \quad (103)$$

After that, the lines can be rearranged according to their momenta. The first part of the subtraction term in this partial fraction decomposition is shown in Fig. 4 on the right hand side. For the other part, $m_{1;1}$ has to be replaced by $m_{2;1}$.

6 Numerical integration

After having performed all other integrations analytically, only the two integrations over k_0^0 and l_0^0 are left. The integration region is given by the factors $B_{n;m}^{k,l}$ which read

$$B_{n;m}^{k,l} = 4^{-2} [(k_0^0 + l_0^0) (n) (m) + (k_0^0 - l_0^0) (n) (m)] : \quad (104)$$

depending on the linearizations $k_0 = k_0^0 - k_1$ and $l_0 = l_0^0 - l_1$. If we take into account that

$$\begin{aligned} 1 &= 2(k_0^0 + E_1 - q_1); & 2 &= 2(k_0^0 - E_2 - q_1); & 3 &= 2k_0^0 \\ 4 &= 2(l_0^0 - E_1 - q_1); & 5 &= 2(l_0^0 + E_2 - q_1); & 6 &= 2l_0^0; \end{aligned} \quad (105)$$

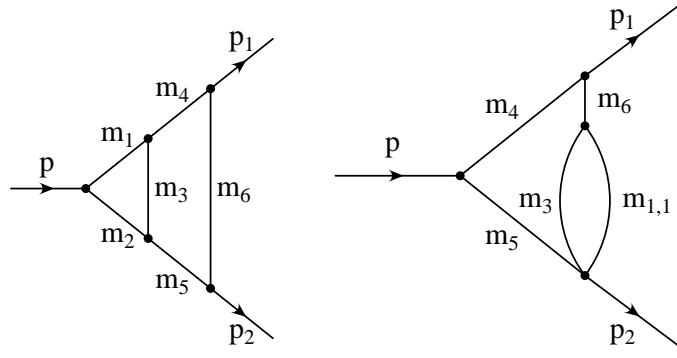


Figure 4: Planar topology T^0 (left hand side) and one part of the partial fraction decomposition of the subtraction term (right hand side)

the integration regions can be seen to be triangles which are bound by the o -diagonal $k_0^0 + l_0^0 = 0$ and the different inequalities coming from n and m . In the cases $(n;m) = (1;4); (2;5); (0;6)$ the integration region vanishes identically. The non-vanishing integration regions are shown in Fig. 5 in case of the linearizations $k_0 = k_0^0 + k_1$ and $l_0 = l_0^0 + l_1$. Two remarks are in order at this point.

Special care has to be taken for the case $(n;m) = (0;6)$. In this case, the integration region vanishes only in the limit $\epsilon_i; \epsilon_i \rightarrow 0$. However, we have thoroughly checked that in this limit the integrand does not diverge, i.e. the integral does not give a non-vanishing contribution even with vanishing integration region [57].

In case that one of the masses vanishes, integration regions vanish in addition. In Fig. 5 we see that if $E_1 = q_z$, i.e. if $p_1^2 = 0$, the triangles $(n;m) = (1;6); (0;4)$ vanish. In case of the opposite linearization and with $p_2^2 = 0$, the same holds for $(n;m) = (2;6); (0;5)$ instead.

The integrations are performed using numerical routines like the Monte Carlo integration routine VEGAS [32, 33] and the program Divonne of the library CUBA [34]. In this section we will present a couple of examples in order to demonstrate the reliability of our method.

6.1 The Z^0 decay via top quark loop

As a first example we consider the process where the Z^0 boson couples to a triangle with top quark current (cf. Fig. 6). We started this example already in Eq. (102) and will

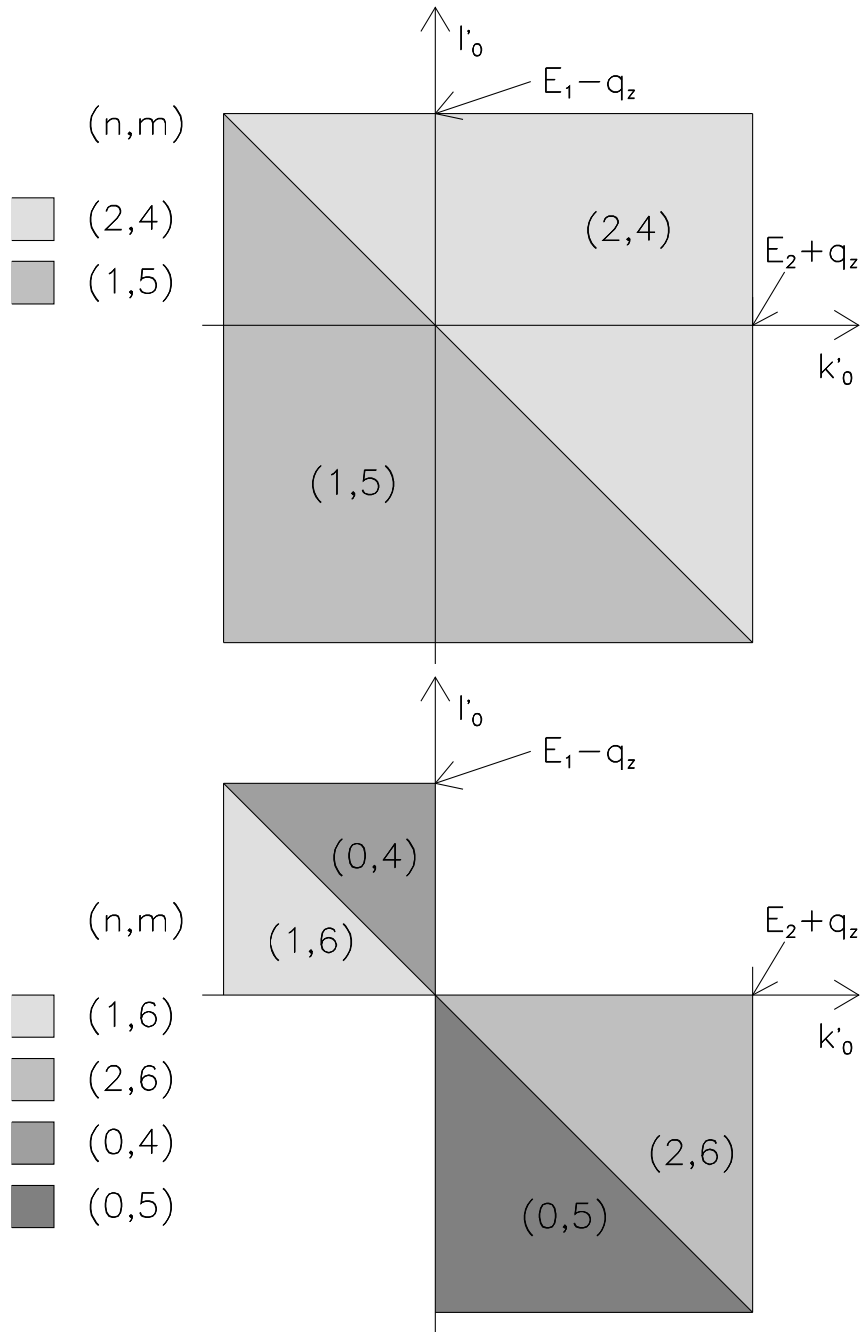


Figure 5: The integration regions for the last (numerical) two-dimensional integration are of the shape of triangles which are bound by the 0 -diagonal $k'_0 + l'_0 = 0$ and two other inequalities. For convenience in two plots instead of one, the integration regions for different values of $(n; m)$ are shown for the linearizations $k_0 = k'_0 + k_1$ and $l_0 = l'_0 + l_1$. In case of the opposite linearizations, the signs in front of the q_z change.

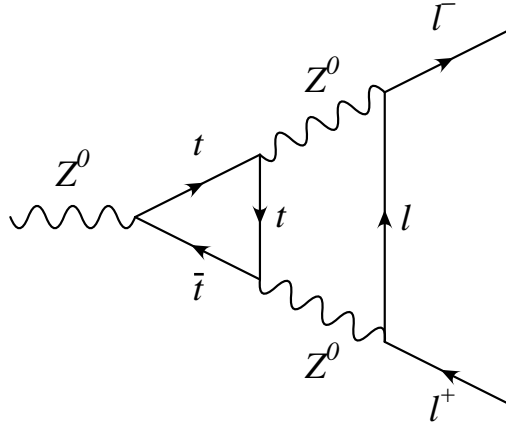


Figure 6: Feynman diagram corresponding to V_2^0 in Eq. (102)

continue at this point. The masses are chosen to be

$$m_1 = m_2 = m_3 = m_t; \quad m_4 = m_5 = m_Z; \quad \text{and} \quad m_6 = m_l \quad (106)$$

where we use the values $m_t = 178 \text{ GeV}$, $m_Z = 91.1876 \text{ GeV}$ [58], and $m_l = 0$. The subtraction masses which should have disjoint values are taken as $m_{1;l} = 150 \text{ GeV}$ and $m_{2;l} = 160 \text{ GeV}$. Because of kinematic reasons, the imaginary part of this integral vanishes.

We calculate the integral for 50 points between $\epsilon_1 = 0.0$ and $\epsilon_1 = 0.5$ for the (dimensionless) parameter ϵ_1 . As a next step we approximate the points by a polynomial with preferably low degree in order to extrapolate to $\epsilon_1 = 0$. The result of this extrapolation can then be compared with the result for the integral where we used $\epsilon_1 = 0$ from the very beginning. For the integration with VEGAS, 260 000 internal points are used, whereas for Divonne we use a standard precision of 10^{-3} . The results of this test are shown in Tables 1 and 2. If $\epsilon_1 = 0$ is used from the very beginning and all integrations are done analytically except for the last two one, we obtain the results shown in the last lines of Tables 1 and 2 and marked with a "x". Obviously, these values are already reliably approximated by the second order test. In case of VEGAS, the quantity $\epsilon^2 = (n-1)$ which is a measure for the reliability of the numerical integration, approaches the optimal value 1.0 quite fast. The deviation of the order of 1 in case of Divonne does not worry because we use this second method only to check the VEGAS calculation. The result is shown graphically in Fig. 7. In this figure we show the results of the numerical calculation in dependence on ϵ_1 together with the result for the semi-analytical calculation for $\epsilon_1 = 0$. The error bars for the latter

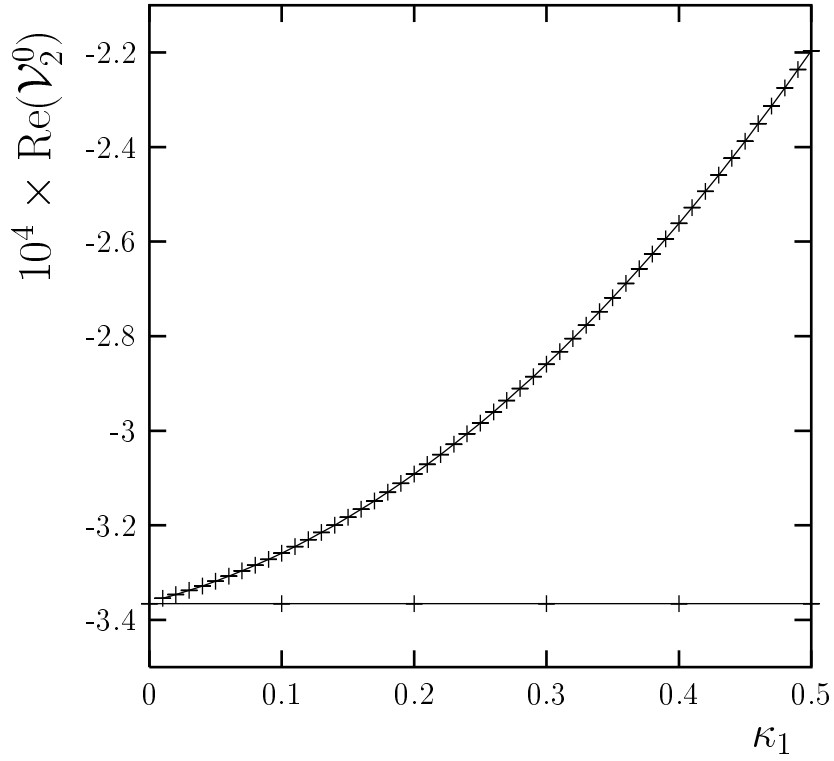


Figure 7: Real part of the integral \mathcal{V}_2^0 in Eq. (102) in dependence on the parameter κ_1 . For the masses and momenta we used values related to the decay of the Z^0 boson into a top-quark loop, as explained in the text (cf. Fig. 6). Shown are the results for the numerical calculation (curve) and the result for the semi-analytical calculation with $\kappa_1 = 0$ (horizontal straight line), both obtained by using VEGAS.

degree	real part	Re	$\frac{2}{\text{Re}} = (n-1)$
0	2:941141	10^0	$1:4 \cdot 10^0$
1	3:484637	10^0	$2:6 \cdot 10^0$
2	3:361064	10^0	$3:9 \cdot 10^0$
3	3:361950	10^0	$5:2 \cdot 10^0$
4	3:361836	10^0	$6:8 \cdot 10^0$
5	3:361884	10^0	$8:6 \cdot 10^0$
6	3:361693	10^0	$1:1 \cdot 10^0$
x	3:365555	10^0	$7:2 \cdot 10^0$

Table 1: Extrapolation of the contributions for V_2^0 using VEGAS

degree	real part	Re	$\frac{2}{\text{Re}} = (n-1)$
0	2:81249	10^0	$3:9 \cdot 10^0$
1	3:52842	10^0	$8:7 \cdot 10^0$
2	3:36111	10^0	$1:3 \cdot 10^0$
3	3:36265	10^0	$1:9 \cdot 10^0$
4	3:36301	10^0	$2:5 \cdot 10^0$
5	3:36294	10^0	$3:2 \cdot 10^0$
6	3:36209	10^0	$4:1 \cdot 10^0$
x	3:36530	10^0	$3:3 \cdot 10^0$

Table 2: Extrapolation of the contributions for V_2^0 using Divonne

are plotted at different points in order to allow for better comparison. Also optically the results for numerical and semi-analytical calculation match very well. This gives us a first piece of confidence in the correct implementation of the algorithm.

6.2 Rotated reduced planar topology

As next we consider the numerical results for a specific example of the rotated reduced planar topology T^5 . The physical starting point is a decay of the Z^0 boson via a lepton loop, coupling to the outer lepton and anti-lepton legs via W bosons. The integral

$$V_{21}^5 = \int \frac{(k_0 + k_1)^2 (l_0 + l_1)}{P_1 P_2 P_3 P_4 P_6} \frac{1}{P_{1;i} P_{2;i}} \frac{1}{P_{4;j}} d^4 k d^4 l \quad (107)$$

contains two subtraction terms, for the k -loop as well as for the l -loop. In this case we consider the limit $\epsilon_1 = 0, \epsilon_2 = 0$. The masses take the values $m_1 = m_2 = m_3 = m_4 = 0$, $m_5 = m_W = 80.425 \text{ GeV}$ [58], and $m_6 = m_l = 0$. The momenta are given by $p_1^2 =$

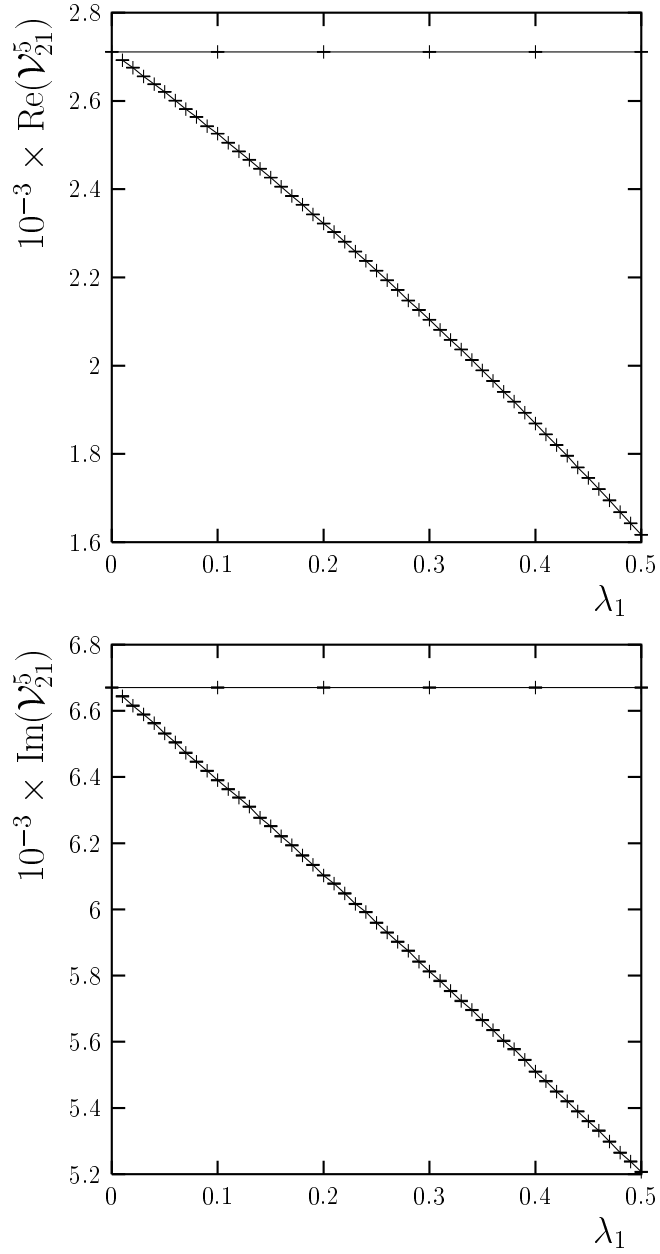


Figure 8: Realpart (top) and imaginary part (bottom) of the integral \mathcal{V}_{21}^5 in Eq. (107) in dependence on the coupled parameters $\lambda_1 = 0:0.5$. Shown are the results for the numerical calculation (curve) and for the semi-analytical calculation with $\lambda_1 = \lambda_2 = 0$ (horizontal straight line), both obtained by using VEGAS.

degree	real part	Re	$\frac{2}{\text{Re}} = (n-1)$	imag. part	Im	$\frac{2}{\text{Im}} = (n-1)$
2	2:71015	3:0	10 ¹	6:67079	7:7	10 ¹
3	2:71047	4:2	10 ¹	6:6712	1:1	10 ¹
x	2:71125	7:0	10 ¹	6:6703	1:7	10 ¹

Table 3: Extrapolation of the contributions for V_{21}^5 using VEGAS

degree	real part	Re	$\frac{2}{\text{Re}} = (n-1)$	imag. part	Im	$\frac{2}{\text{Im}} = (n-1)$
2	2:7094	1:0	10 ¹	6:6691	2:7	10 ¹
x	2:7042	2:6	10 ¹	6:6736	6:6	10 ¹

Table 4: Extrapolation of the contributions for V_{21}^5 using D ivonne

$\frac{1}{p^2} = m_1 = 0$ and $\frac{1}{p^2} = m_Z$. For the three subtraction masses we take $m_{1;1} = 100 \text{ GeV}$, $m_{2;1} = 300 \text{ GeV}$, and $m_{4;1} = 110 \text{ GeV}$. In Table 3 the results for the numerical integration with VEGAS are shown for the real and the imaginary part. Because we have the cross-check with D ivonne at hand, we show only the most reliable values at polynomial degrees 2 and 3. For the results obtained by using D ivonne (Table 4) a single value is shown. The results for the semi-analytical calculation are again given in the last lines of the two tables. Looking at the values obtained by using VEGAS in Fig. 8, we realize very good agreement.

6.3 Results for tuned decay mass

For the integral with two subtractions for the k-loop,

$$V_3^0 = \int \frac{(k_0 - k_1)^3 d^4 k d^4 l Y^2}{P_1 P_2 P_3 P_4 P_5 P_6} \frac{1}{P_{1;1} P_{2;1}} ; \quad (108)$$

we tune the decay mass $M = \frac{1}{p^2}$ in order to identify different thresholds. The values for masses and outgoing momenta are again taken from Eq. (101). In tuning M we can observe the behaviour of the real and the imaginary part. The behaviour is shown in Fig. 9 for decay mass values close to $M = 320 \text{ GeV}$. As in case of the simple example shown in Fig. 3 we notice a vertical incline at the point $M = 320 \text{ GeV}$ which corresponds to the two-particle threshold $M^2 = p^2 = (m_4 + m_5)^2$. In a second step we are looking more closely at the threshold region. Taking the value $M = 325 \text{ GeV}$, we analyze the real and imaginary parts for $\epsilon_1 \neq 0$. In Table 5 we show results of the polynomial fit for the results obtained by VEGAS. The last line of Table 5 and the single line of Table 6 are the semi-analytic

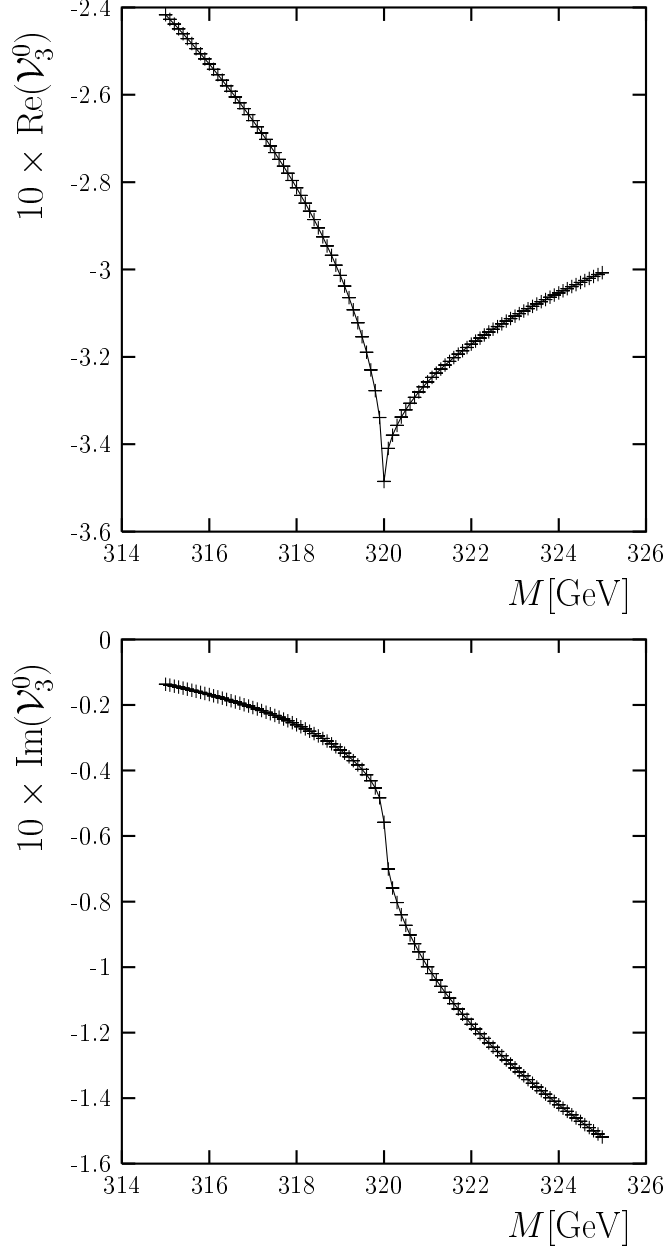


Figure 9: Realpart (top) and imaginary part (bottom) of the integral V_3^0 in Eq. (108) in dependence on the decay mass $M = \sqrt{p^2}$ close to $M = 320 \text{ GeV}$. The values for masses and outgoing momenta are taken from Eq. (101).

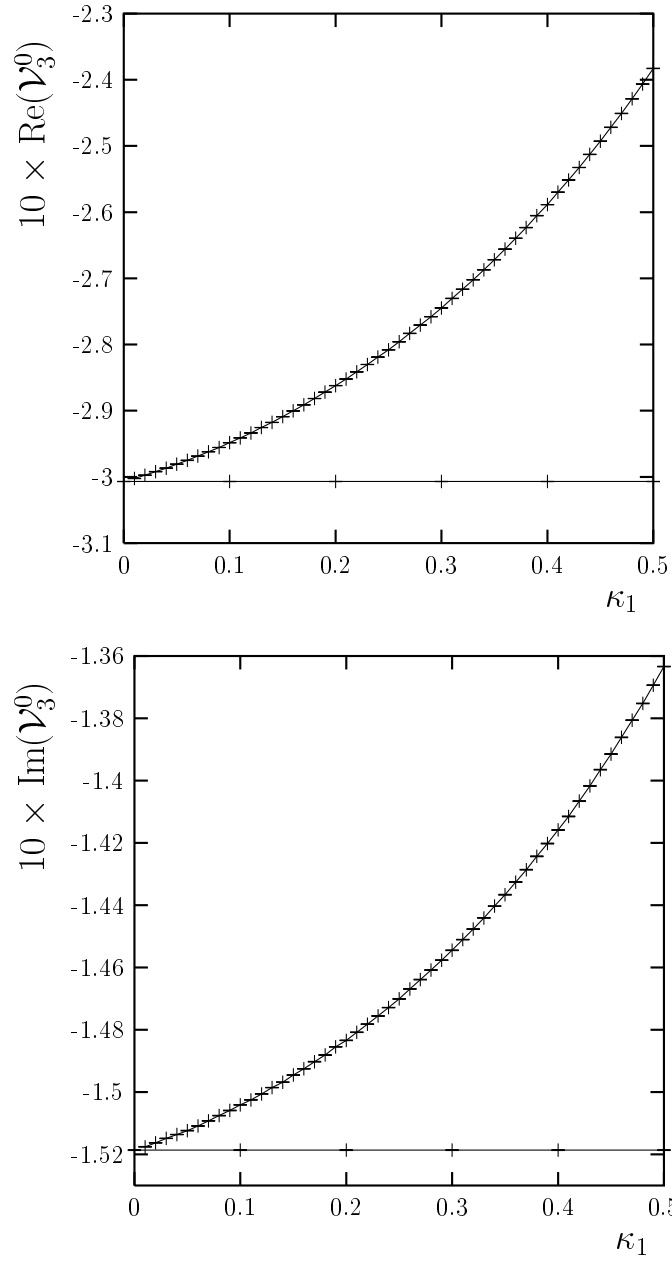


Figure 10: Real part (top) and imaginary part (bottom) of the integral V_3^0 in Eq. (108) in dependence on the coupled parameters $\kappa_2 = 0:0.6$ for the decay mass value $M = \sqrt{p^2} = 325 \text{ GeV}$. Shown are the results for the numerical calculation (curve) and for the semi-analytical calculation with $\kappa_2 = \kappa_1 = 0$ (horizontal straight line), both obtained by using VEGAS.

degree	real part	Re	$\frac{2}{\text{Re}} = (n-1)$	imag. part	Im	$\frac{2}{\text{Im}} = (n-1)$
3	3.00814	10^{-1}	$1.2 \cdot 10^5$	1.519135	10^{-1}	$5.2 \cdot 10^6$
4	3.00692	10^{-1}	$1.5 \cdot 10^5$	1.518660	10^{-1}	$6.8 \cdot 10^6$
x	3.00689	10^{-1}	$1.7 \cdot 10^5$	1.51865	10^{-1}	$1.4 \cdot 10^6$

Table 5: Extrapolation of the contributions for V_3^0 using VEGAS

degree	real part	Re	$\frac{2}{\text{Re}} = (n-1)$	imag. part	Im	$\frac{2}{\text{Im}} = (n-1)$
x	3.0083	10^{-1}	$2.9 \cdot 10^4$	1.5196	10^{-1}	$1.4 \cdot 10^4$

Table 6: Extrapolation of the contributions for V_3^0 using Divonne

results obtained by using VEGAS and Divonne, respectively. The results are shown in Fig. 10. Again we could convince ourselves that both methods lead to the same result in the limit $n \rightarrow 0$.

6.4 Combined integration

After having performed these tests we are convinced that it is possible to evaluate semi-automatically the partial results from the different master integrals. This might be done by performing the numerical integrations separately for each master integral and afterwards combining the results. However, it turns out that the more stable method is to first perform the analytical integration and do the numerical integration for the sum of all basic integrands relevant for the given process. This is especially true for values on the threshold or close to it. As an example we use

$$T_{\text{ex}} = \int \frac{(k_1)(p_1 k)(p_2 k + p_2 l)}{P_1 P_2 P_3 P_4 P_5 P_6} d^4 k d^4 l \quad (109)$$

After the tensor reduction explained in Sec. 3, besides of simpler topologies we are left with the original planar topology and the two rotated reduced planar topologies, both with different powers of $(k_0 - k_1)$ and $(l_0 - l_1)$. These master integrals can be calculated by applying the subtractions explained in Sec. 4. For the convergent part, the limit $n \rightarrow 0$ can be performed. All integrations up to the last two one can be done analytically. The combination of different results at this point shall be called V_{ex} . As explained before, we can now proceed either in combining all analytical results to a single expression and integrate this expression numerically (combined integration), or in performing the numerical integration of the analytical expression for each of the master integrals separately and add

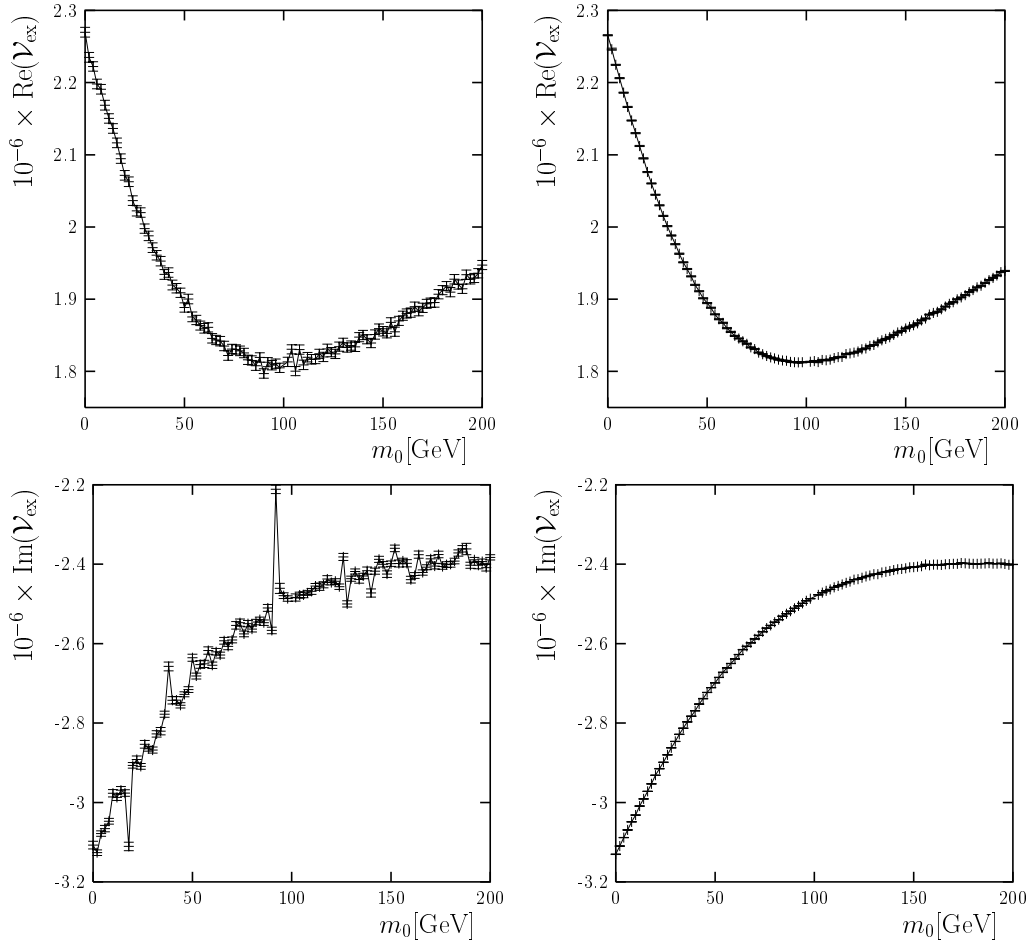


Figure 11: Real part (top) and imaginary part (bottom) of the integral V_{ex} in dependence on the mass parameter m_0 of the subtraction masses for the decay mass value on the two-particle threshold at $M = \sqrt{p^2} = 500 \text{ GeV}$. Shown are the results for separated (left hand side) and combined numerical integration (right hand side) with VEGAS.

up the results afterwards (separated integration). We will perform both calculations in the following to compare them.

For the physical masses and outgoing momenta we again use the values in Eq. (101). The decay mass $M = \sqrt{p^2} = 500 \text{ GeV}$ is placed on the two-particle threshold $p^2 = (m_5 + m_6)^2$. In order to compare dependencies, for the subtraction masses we take values with an offset m_0 which in this example runs from 0 GeV to 200 GeV ,⁵

$$\begin{aligned} m_{1;1} &= 5 \text{ GeV} + m_0 & m_{1;2} &= 25 \text{ GeV} + m_0 \\ m_{2;1} &= 15 \text{ GeV} + m_0 & m_{2;2} &= 35 \text{ GeV} + m_0 : \end{aligned} \tag{110}$$

The results are shown in Fig. 11. The left hand side of Fig. 11 shows real and imaginary parts for the separated integration, the right hand side shows real and imaginary parts for the combined integration. It is obvious that the combined integration is much more stable.

7 Conclusions

Using the parallel/orthogonal space method, we elaborated a new method to calculate the planar and rotated planar ladder two-loop three-point diagrams in the general massive case. Our method does not depend on a specific physical decay process but is suitable to calculate all planar two-loop vertex diagrams which may arise in the standard model of electroweak interactions.

We presented a tensor reduction which reduces the mentioned topologies with arbitrary tensor structure to a set of master integrals with strongly restricted, well-defined numerator structure. For the semi-analytical calculation of the UV-finite part of those master integrals which have the same topologies after tensor reduction, we developed and implemented an algorithm. While most of the calculations are done analytically, for the remaining two integrations we used different numerical methods.

The integration of the important basic integrals was checked exhaustively in the limit of vanishing subtraction parameters by comparing the semi-analytical calculation with results of a numerical integration. The numerical integration as the final step of the semi-analytical calculation turns out to be stable. This is valid especially in the case where the numerical integration is done not for each basic integral separately but for the sum of all analytical results necessary for the given process.

⁵Note that V_{ex} still does not need to be independent of the subtraction masses because only in the sum with the finite parts of the subtraction terms this dependence will vanish.

For the remaining basic integrals and subtraction terms with simpler topologies there are already other methods established. In part, these methods are already implemented in *χloops*. Therefore, in writing links to existing codes, these cases can easily be implemented into our calculations. The still missing topologies are two-loop three-point topologies containing a two-point subloop. These parts still have to be implemented [49, 50].

Finally, our method can easily be extended to the non-planar two-loop vertex topology. As far as possible, the computer codes written in the course of the project are developed and implemented for most general processes. Because of this, we plan to include our calculations in the *χloops* project in the near future.

Acknowledgements

We thank H. S. Do, A. v. Hameren, M. Rogal, K. Schilcher and H. Spiesberger for helpful discussions. M. K. wants to thank C. Bauer and J. Vulliamy for computer-technical support. S. G. acknowledges support by the DFG as a guest scientist in Mainz, by the Estonian targeted project No. 0182647s04, and by the grant No. 6216 given by the Estonian Science Foundation. M. K. was supported in parts by the BMBF and by the Graduiertenkolleg "Eichtheorien { experimentelle Tests und theoretische Grundlagen", Mainz University.

A Basic integrals

In this appendix we list the analytical results for the basic integrals in Eq. (90) in terms of the parameters $r_s, r_t, r_0, s_0,$ and t_0 . In order to calculate these integrals, we introduce cut-offs ϵ_s and ϵ_t . The results depending on these cut-offs are extremely long and contain products of logarithms and dilogarithms [57]. However, we can show that these divergences cancel in the differences which always occur in practice. In order to get the reader familiar with these features, we explain the calculation for the simplest example.

A.1 The integral $F_{0;0}^{st}$

The regularized integral is given by

$$\begin{aligned}
 F_{0;0}^{st} &= \int_0^{\epsilon_t} dt \int_0^{\epsilon_s} ds \frac{1}{c \sqrt{(r_0 - \epsilon_s r_t)^2 + 4st}} \\
 &= \frac{\epsilon_t}{r_s} \ln \frac{r_s r_0 + (2 - \epsilon_s r_t) \epsilon_t}{2(r_s r_0 + (1 - \epsilon_s r_t) \epsilon_t)} + \frac{\epsilon_s}{r_t} \ln \frac{r_t r_0 + (2 - \epsilon_s r_t) \epsilon_s}{2(r_t r_0 + (1 - \epsilon_s r_t) \epsilon_s)} \\
 &\quad + \frac{r_0}{1 - \epsilon_s r_t} \ln \epsilon_t + \frac{r_s r_0}{1 - \epsilon_s r_t} + \ln \epsilon_s + \frac{r_t r_0}{1 - \epsilon_s r_t} + i \pi \\
 &\quad - \ln \left[(1 + \epsilon_s r_t) + (1 - \epsilon_s r_t) (\epsilon_s \epsilon_t + r_t \epsilon_t + \epsilon_s) \right] \ln \frac{r_0}{2(1 - \epsilon_s r_t)^2} \quad ! \quad (A 1)
 \end{aligned}$$

where

$$\epsilon = \frac{q}{(r_0 - \epsilon_s r_t)^2 + 4 \epsilon_s \epsilon_t} \quad (A 2)$$

What to do with the singularity? As a first step we can separate the divergent part which depends on ϵ_s, ϵ_t and ϵ from the convergent part. But how does the divergent part cancel? If we look at Eq. (88) where $F_{0;0}^{st}$ appears, we see that it actually appears as part of a sum. If we concentrate on the summation over n and consider how $N_{1;ija}^k$ and $N_{2;ija}^k$ are defined in Eqs. (53) and (54), we see that the replacement of $n = 1$ by $n = 2$ causes simply the flip of the sign. The same is valid for $N_{1;jjb}^1$ and $N_{2;jjb}^1$. Therefore, an expression which is of relevance for the subtracted integrals is the sum

$$\sum_{n=1}^{\infty} \sum_{m=x/6}^{\infty} (-1)^{n+m} F_{0;0}^{st}(r_s; r_t; r_{n,ijm}; j): \quad (A 3)$$

In replacing ϵ_s by ϵ_s^0 and ϵ_t by ϵ_t^0 with $\epsilon_s^0 = \epsilon_t^0 = 1$ we indeed can show that

$$\sum_{n=1}^{\infty} \sum_{m=x/6}^{\infty} (-1)^{n+m} F_{0;0}^{st,div}(r_s; r_t; r_{n,ijm}; j) = O(\epsilon_s^0 \epsilon_t^0): \quad (A 4)$$

For $\epsilon \neq 0$, therefore, the divergent part will cancel in the difference. We only have to consider the convergent part

$$F_{0;0}^{st;conv} = \frac{r_0}{1 - \epsilon r_t} \sum_{i=0}^{\infty} \binom{i}{\epsilon} \ln \frac{r_0}{2(1 - \epsilon r_t)^2} \quad (A 5)$$

Finally, we see that

$$\sum_{n=1}^{\infty} \sum_{m=x;6}^{\infty} (1)^{n+m} r_{n,i;m} r_{j} \sum_{0}^{\infty} \sum_{m=x;6}^{\infty} (1)^{i+j} = 0 \quad (A 6)$$

(cf. Eq. (91) including remarks given there). Therefore, we can skip all terms which are linear in r_0 . The result which we have to implement is

$$F_{0;0}^{st;impl} = \frac{r_0}{1 - \epsilon r_t} \sum_{i=0}^{\infty} \binom{i}{\epsilon} \ln \binom{j}{\epsilon} \quad (A 7)$$

In the following we will only give results which are to be implemented. For the integrals with one index we will show only results for F^s . Results for F^t can easily be obtained by replacing $s_0 \leftrightarrow t_0$ and $r_s \leftrightarrow r_t$.

A.2 The integrals F^s

$$r_s F_0^{s;impl} = \text{Re Li}_2 \left(1 + \frac{r_s r_0}{t_0 (1 - \epsilon r_t)} \right) + i \sum_{i=0}^{\infty} \binom{i}{\epsilon} \ln \left(1 + \frac{r_s r_0}{t_0 (1 - \epsilon r_t)} \right) \sum_{j=0}^{\infty} \binom{j}{\epsilon} \ln t_0 + \frac{r_s r_0}{1 - \epsilon r_t} \quad (A 8)$$

$$r_s F_1^{s;impl} = (2 - \epsilon r_t) \frac{r_s r_0}{1 - \epsilon r_t} \ln \binom{j_0}{\epsilon} + t_0 + \frac{r_s r_0}{2 - \epsilon r_t} \text{Re Li}_2 \left(1 + \frac{r_s r_0}{t_0 (1 - \epsilon r_t)} \right) + i (2 - \epsilon r_t) \sum_{i=0}^{\infty} \binom{i}{\epsilon} \frac{r_s r_0}{1 - \epsilon r_t} \sum_{j=0}^{\infty} \binom{j}{\epsilon} \ln \left(1 + \frac{r_s r_0}{t_0 (1 - \epsilon r_t)} \right) + ((2 - \epsilon r_t)t_0 + r_s r_0) \sum_{i=0}^{\infty} \binom{i}{\epsilon} \ln t_0 + \frac{r_s r_0}{1 - \epsilon r_t} \quad (A 9)$$

$$r_s F_2^{s;impl} = \left(\frac{1}{2} \frac{r_s r_0}{1 - \epsilon r_t} \sum_{i=0}^{\infty} \binom{i}{\epsilon} (6 - 6\epsilon r_t + r_s^2 r_t^2) \right) + \frac{r_s r_0}{1 - \epsilon r_t} \sum_{i=0}^{\infty} \binom{i}{\epsilon} (6 - 6\epsilon r_t + r_s^2 r_t^2) t_0 + 2(3 - \epsilon r_t) r_s r_0 \sum_{i=0}^{\infty} \binom{i}{\epsilon} \ln \binom{j_0}{\epsilon} + (6 - 6\epsilon r_t + r_s^2 r_t^2) t_0^2 + 2(3 - \epsilon r_t) r_s r_0 t_0 + r_s^2 r_0^2 \text{Re Li}_2 \left(1 + \frac{r_s r_0}{t_0 (1 - \epsilon r_t)} \right) \quad (A 10)$$

$$\begin{aligned}
& i \quad (6) \quad \frac{1}{2} \frac{r_s r_0}{1 - r_s r_t} (6 - 6r_s r_t + r_s^2 r_t^2) \\
& \quad \frac{r_s r_0}{1 - r_s r_t} (6 - 6r_s r_t + r_s^2 r_t^2) t_0 + 2(3 - r_s r_t) r_s r_0 \\
& + (6 - 6r_s r_t + r_s^2 r_t^2) t_0^2 + 2(3 - r_s r_t) r_s r_0 t_0 + r_s^2 r_0^2 \ln \left(1 + \frac{r_s r_0}{t_0 (1 - r_s r_t)} \right) \\
& (t) \quad (6 - 6r_s r_t + r_s^2 r_t^2) t_0^2 + 2(3 - r_s r_t) r_s r_0 t_0 + r_s^2 r_0^2 \ln \left(t_0 + \frac{r_s r_0}{1 - r_s r_t} \right)
\end{aligned} \tag{A 10}$$

While the integral $F_{0,0}^{st}$ is used for illustrative reasons only but does not appear in calculations because the integration region vanishes, it figures out that the integrals F^s and F^t are sufficient for calculations within the standard model of electroweak interactions using Feynman gauge.

References

- [1] W. Hollik, G. Duckeck, "Electroweak Precision Tests at LEP", Springer 2000
- [2] D.Y. Bardin, J. Phys. G 29 (2003) 75
- [3] W. Hollik et al., Acta Phys. Polon. B 35 (2004) 2533
- [4] [LEP Collaborations], Report No. LEPEW WG/2004-01, CERN-PH-EP/2004-069 (Dec 2004) [arXiv:hep-ex/0412015]
- [5] J.A. Aguilar-Saavedra et al. [ECFA/DESY LC Physics Working Group], "TESLA Technical Design Report Part III: Physics at an e^+e^- Linear Collider", Report No. DESY-TESLA-2001-23 [arXiv:hep-ph/0106315]
- [6] S. Heinemeyer and G. Weiglein, "Electroweak precision tests with GigaZ", published in Batavia 2000, Physics and experiments with future linear e^+e^- colliders, pp. 511-514, Report No. LC-TH-2001-001 [arXiv:hep-ph/0012364]
- [7] G. Weiglein, Eur. Phys. J. C 33 (2004) S630
- [8] G. Weiglein et al. [LHC/LC Study Group], "Physics interplay of the LHC and the ILC", Report No. SLAC-PUB-10764 [arXiv:hep-ph/0410364]

- [9] S. Heineneyer, "Loop calculations: Summary",
Report no. CERN-TH-2004-159 [arXiv:hep-ph/0408269]
- [10] D. Kreimer, Phys. Lett. B 292 (1992) 341
- [11] N. I. Usyukina and A. I. Davydychev, Phys. Lett. B 348 (1995) 503
- [12] A. I. Davydychev and J. B. Tausk, Nucl. Phys. B 465 (1996) 507
- [13] J. Fujimoto, Y. Shimizu, K. Kato and T. Kaneko, Int. J. Mod. Phys. C 6 (1995) 525
- [14] A. A. Pivovarov, Phys. Atom. Nucl. 63 (2000) 1646 [Yad. Fiz. 63N 9 (2000) 1734]
[arXiv:hep-ph/9905485].
- [15] K. G. Chetyrkin, R. Harlander, J. H. Kuhn and M. Steinhauser,
Nucl. Instrum. Meth. A 389 (1997) 354
- [16] S. G. Rothe, J. G. Körner and A. A. Pivovarov, Phys. Lett. B 443 (1998) 269; Nucl. Phys.
B 542 (1999) 515; Eur. Phys. J. C 11 (1999) 279; Phys. Rev. D 60 (1999) 061701;
Phys. Rev. D 61 (2000) 071501; Phys. Rev. D 65 (2002) 036001; Eur. Phys. J.
C 36 (2004) 471; "On the evaluation of a certain class of Feynman diagrams in
x-space: Sunrise-type topologies at any loop order," Report No. MZ-TH-05-08
[arXiv:hep-ph/0506286]; S. G. Rothe and A. A. Pivovarov, Nucl. Phys. B 580 (2000)
459
- [17] A. Ghinculov and Y. P. Yao, Phys. Rev. D 63 (2001) 054510
- [18] A. I. Davydychev and V. A. Smirnov, Nucl. Instrum. Meth. A 502 (2003) 621
- [19] R. Bonciani, P. Mastrolia and E. Remiddi, Nucl. Phys. B 676 (2004) 399
- [20] H. S. Do, Dissertation, Mainz University, 2003
- [21] G. Passarino, Nucl. Phys. B 619 (2001) 257
- [22] A. Ferroglia, M. Passera, G. Passarino and S. Uccirati,
Nucl. Phys. B 680 (2004) 199 [arXiv:hep-ph/0311186].
- [23] S. Actis, A. Ferroglia, G. Passarino, M. Passera and S. Uccirati,
Nucl. Phys. B 703 (2004) 3

- [24] M .A w ram ik, M .C zakon, A .Freitas and G .W eiglein,
Phys. Rev. Lett. 93 (2004) 201805; Nucl. Phys. Proc. Suppl. 135 (2004) 119
- [25] W .H ollik, U .M eier and S .U ccirati, Report No. M P P -2005-77 [arX iv hep-ph/0507158]
- [26] D .K rein er, Phys. Atom . Nucl. 56 (1993) 1546
- [27] D .K rein er, Mod. Phys. Lett. A 9 (1994) 1105
- [28] A .V .K otikov, Phys. Lett. B 259 (1991) 314
- [29] J .F leischer, A .V .K otikov and O .L .Veretin,
Phys. Lett. B 417 (1998) 163; Nucl. Phys. B 547 (1999) 343
- [30] V .A .Sm imov and E .R .R akh m etov,
Theor. Math. Phys. 120 (1999) 870 [Teor. Mat. Fiz. 120 (1999) 64]
- [31] T .G .B irthw right, E .W .N .G lover and P .M arquard, JHEP 0409 (2004) 042
- [32] G .P .Lepage, " Vegas: An Adaptive Multidimensional Integration Program ",
Report No. CLNS-80/447
- [33] T .O hl, Comput. Phys. Commun. 120 (1999) 13
- [34] T .H ahn, " CUBA :A library for multidimensional numerical integration ",
Report No. M P P -2004-40 [arX iv hep-ph/0404043]
- [35] D .K rein er, Nucl. Instrum .M eth. A 389 (1997) 323
- [36] L .B rucher, Nucl. Instrum .M eth. A 389 (1997) 327
- [37] J .F ranzkow ski, Nucl. Instrum .M eth. A 389 (1997) 333
- [38] A .F rink, J .G .K omer and J .B .Tausk, " Massive two-loop integrals and Higgs physics",
published in the Proceedings of the Joint Particle Physics Meeting, O uranoupolis,
G reece, M ay 1997, pp. 175{200
- [39] C .B auer and H .S .D o, Comput. Phys. Commun. 144 (2002) 154
- [40] C .B auer, A .F rink and R .K reckel, Report No. M Z -TH /00-17 [arX iv:cs.sc/0004015]

- [41] D . K reim er, Z . P hys. C 54 (1992) 667
- [42] D . K reim er, Int. J. M od. P hys. A 8 (1993) 1797
- [43] A . C zamecki, U . K ilian and D . K reim er, Nucl. P hys. B 433 (1995) 259
- [44] A . F rink, D iplom a thesis, M ainz U niversity, 1996
- [45] A . F rink, U . K ilian and D . K reim er, Nucl. P hys. B 488 (1997) 426
- [46] A . F rink, D issertation, M ainz U niversity, 2000
- [47] G . P assarino and M . J . G . V eltm an, Nucl. P hys. B 160 (1979) 151
- [48] S . B auberger, F A . B erends, M . B ohm and M . B uza, Nucl. P hys. B 434 (1995) 383
- [49] S . B auberger, M . B ohm , G . W eiglein, F A . B erends and M . B uza,
Nucl. P hys. P roc. Suppl. 37B (1994) 95
- [50] P . P ost, D issertation, M ainz U niversity, 1997
- [51] J . F leischer, V A . S m imov, A . F rink, J . G . K omer, D . K reim er, K . S childer and
J B . T ausk, Eur. P hys. J. C 2 (1998) 747
- [52] R . H arlander and M . S teinhauser, P rog. P art. Nucl. P hys. 43 (1999) 167
- [53] U . K ilian, D issertation, M ainz U niversity, 1996
- [54] L D . L andau, Nucl. P hys. 13 (1959) 181
- [55] M . B ohm , A . D enner, H . J oos,
"G auge T heory of the Strong and E lectroweak Interaction", Teubner, 2001
- [56] R E . C utkosky, J. M ath. P hys. 1 (1960) 429
- [57] M M . K nodel, D issertation, M ainz U niversity, 2005
- [58] S . E idelm an et al. [P article D ata G roup], P hys. Lett. B 592 (2004) 1